

1 **Identification of the source of dolerites used at the Waun Mawn**
2 **stone circle in the Mynydd Preseli, west Wales and implications for**
3 **the proposed link with Stonehenge**

4
5 **Richard E. Bevins^{a,b,*}, Nick J.G. Pearce^b, Mike Parker Pearson^c, Rob A. Ixer^c**
6

7 ^a*Department of Natural Sciences, National Museum of Wales, Cathays Park, Cardiff CF10*
8 *3NP, UK*

9 ^b*Department of Geography and Earth Sciences, Aberystwyth University, Aberystwyth SY23*
10 *3DB, UK*

11 ^c*Institute of Archaeology, University College London, London WC1H 0PY, UK*
12

13 * Author for correspondence: Richard Bevins, Email:

14 richard.bevins@honorary.museumwales.ac.uk
15
16

17 Keywords: Waun Mawn, stone circle, Mynydd Preseli, Wales, dolerite, Stonehenge
18

19 Conflict of interest: The authors have no conflicts of interest
20

21 **Abstract**

22 A Neolithic stone circle at Waun Mawn, in the Mynydd Preseli, west Wales, has been
23 proposed as the original location of some dolerite megaliths at Stonehenge, including one
24 known as Stone 62. To investigate this hypothesis, *in-situ* analyses, using a portable XRF,
25 have been obtained for four extant non-spotted doleritic monoliths at Waun Mawn, along
26 with two weathered doleritic fragments from a stonehole (number 91). The data obtained
27 have been compared to data from spotted and non-spotted dolerite outcrops across the
28 Mynydd Preseli, an area known to be the source of some Stonehenge doleritic bluestones,
29 as well as data from *in-situ* analysis of Stone 62 (non-spotted dolerite) and *ex-situ* analysis of
30 a core taken from Stone 62 in the late 1980's.

31 Recently, Stone 62 has been identified as coming from Garn Ddu Fach, an outcrop some
32 6.79 km to the east-southeast of Waun Mawn. None of the four dolerite monoliths at Waun
33 Mawn have compositions which match Stonehenge Stone 62, and neither do the weathered
34 fragments from stonehole 91. Rather the data show that the Waun Mawn monoliths, and
35 most probably the weathered stonehole fragments, can be sourced to Cerrig Lladron, 2.37
36 km southwest of Waun Mawn, suggesting that a very local stone source was used in
37 construction of the Waun Mawn stone circle. It is noted that there is evidence that at least
38 eight stones had been erected and subsequently removed from the Waun Mawn circle but
39 probability analysis suggests strongly that the missing stones were also derived, at least
40 largely, from Cerrig Lladron.

41

42 **1. Introduction**

43 Stonehenge, lying on Salisbury Plain in Wiltshire, England, is remarkable for the distance
44 its stones have been transported, making it unique amongst European megalithic
45 monuments (Parker Pearson et al., 2020). Its sarsen stones, fifty-two in number and
46 weighing between 4-30 tons comprise the Outer Sarsen Circle, the Sarsen Trilithon
47 Horseshoe and the outlying Station Stones, Slaughter Stone and Heel Stone. Nash et al.
48 (2020) say that 50 of the 52 stones originate from a common source area and most probably
49 came from West Woods, on the edge of the Marlborough Downs some 22.5 km to the north
50 of Stonehenge. However, it is the smaller bluestones, forty-four in number (in 46 pieces)
51 and weighing 1-4 tons, which are even more remarkable as almost all of them have been
52 provenanced to the Mynydd Preseli area in north Pembrokeshire, some 225 km away as the
53 crow flies. Whilst the sarsen stones are all silcretes the bluestones are a lithological
54 assemblage comprising chiefly dolerites and andesitic, dacitic and rhyolitic tuffs, as well as
55 sandstone. Locating exactly where the bluestones come from will provide a better
56 understanding of this iconic and unique monument, possibly leading to a greater
57 appreciation of the reasons behind its construction approximately 5000 years ago.

58 In 2021, following excavation at a partially preserved stone circle at Waun Mawn in the
59 Mynydd Preseli, it was proposed that missing stones had been taken to contribute to the
60 original construction of Stonehenge (Parker Pearson et al., 2021). The excavation appeared
61 in a BBC TV documentary entitled 'Stonehenge: The Lost Circle Revealed' (first broadcast on
62 December 12, 2021), in which Stonehenge was described as 'a second-hand monument' – a
63 phrase quoted by the media around the world. In this paper we present the first geological
64 analysis of the Welsh circle's surviving stones and compare them to material at Stonehenge
65 and to outcrops in north Pembrokeshire.

66 **2. Previous studies**

67 A possible north Pembrokeshire source for the bluestones was first mooted by A.C.
68 Ramsay and colleagues in 1858 but it was H.H. Thomas, a geologist with the then Geological
69 Survey of Great Britain, who provided the first detailed account of the bluestone lithologies
70 in a seminal paper in 1923, assigning the dolerites to Carn Meini and Cerrigmarchogion, the

71 'rhyolites' to Carn Alw and the tuffs to the northern slopes of Foel Drygarn. He was
72 convinced that the majority of the bluestones came from this restricted area towards the
73 eastern extremity of the Mynydd Preseli. Key locations referred to in this paper are shown
74 on Figure 1.

75 Since 2009 we have been undertaking a systematic review of the bluestones, re-
76 examining their lithologies and investigating further their potential sources. The great
77 majority of the rhyolitic debitage recovered from the Stonehenge Landscape was
78 determined by Ixer and Bevins (2010, 2011) and Bevins et al. (2011, 2012) to be from Craig
79 Rhos-y-Felin, an outcrop on low ground to the north of the Mynydd Preseli. In addition,
80 investigations of the detailed mineralogy of the 'Altar Stone' (Stone 80), a grey-green,
81 carbonate-rich sandstone, have suggested that it does not come from the Cosheston Group
82 in the Milford Haven area (see Bevins et al., 2020; Ixer et al., 2020), an earlier proposal
83 which lay behind the notion that the bluestones were transported in part by sea up the
84 Bristol Channel (Atkinson, 1956).

85 It is re-examination of the sources of the dolerites that is pertinent to this paper. The
86 bluestone dolerites comprise spotted and non-spotted varieties, the spots being
87 saussuritized plagioclase phenocrysts/glomerocrysts (Bevins et al., 2021a). Bevins et al.
88 (2014), using standard laboratory-based XRF data generated in the late 1980's, identified
89 three compositional groups, namely Group 1 (spotted, low Ni and Cr), Group 2 (non-
90 spotted, high Ni, low Cr) and Group 3 (spotted, low Ni, high Cr). They suggested that the
91 majority of the spotted dolerites came from Carn Goedog, noting that none in fact matched
92 to Carn Meini, the source proposed by Thomas (1923). Regarding the Group 2 non-spotted
93 dolerites (which includes Stonehenge stones 44, 45 and 62 and debitage fragment OU6)
94 Bevins et al. (2014) suggested that they were derived from either Cerrigmarchogion or Craig
95 Talfynydd. However, using newly generated ICP-MS data, Bevins et al. (2021b) refined
96 slightly the sources of the non-spotted dolerites, concluding that, whilst Stone 45 did indeed
97 come from Cerrigmarchogion, none of the non-spotted bluestone dolerites were sourced
98 from Craig Talfynydd and whilst they were not able to conclusively identify the source of
99 Stone 62 or debitage fragment OU6 they noted a close similarity to non-spotted dolerite
100 from Carn Ddafad-las and Garn Ddu Fach. They were unable to suggest a source for Stone
101 44. In order to investigate further the source of Stone 62, Pearce et al. (2022) undertook *in-*

102 *situ* compositional analysis using portable XRF (pXRF) of that stone at Stonehenge and
103 compared it with analyses by the same method from outcrops in the Mynydd Preseli. Their
104 data showed that analyses from Stone 62 and from the Preseli outcrop Garn Ddu Fach
105 occupied the same compositional space on various binary elemental plots, concluding that
106 Garn Ddu Fach was the likely source of Stonehenge Stone 62.

107 As noted earlier, on the basis of archaeological excavations, Parker Pearson et al. (2021)
108 have recently suggested that Stonehenge Stone 62 was removed from a partial stone circle
109 at Waun Mawn in the Mynydd Preseli (see Figure 1). This has major implications for
110 understanding the potential origins of the bluestones used in the construction of
111 Stonehenge, suggesting that they might first have been used locally in the construction of
112 stone circles which were subsequently dismantled, either completely or at least in part, with
113 stones being transported to and used in the construction of Stonehenge. In order to test
114 this, we have analysed by pXRF dolerite outcrops from across the Mynydd Preseli area,
115 including those closest to Waun Mawn (Cerrig Lladron, Carn Fach and Carnau Ysfa) and
116 compared the results with those from the four extant dolerite monoliths and from two non-
117 spotted dolerite fragments from stonehole 91 at Waun Mawn. We also compare the pXRF
118 data from Stone 62 at Stonehenge with the pXRF data for the four exposed non-spotted
119 dolerite monoliths and the two stonehole fragments at Waun Mawn.

120 **3. Archaeological context**

121 Waun Mawn's four stones (three of them recumbent and one standing) have been
122 considered to be the remains of a stone circle for the last hundred years (RCAHMW, 1925,
123 258–9). The site is located on the slope of a hill on the north side of the Mynydd Preseli
124 ridge, about 3.9 and 4.6 km respectively from the bluestone sources of Craig Rhos-y-Felin
125 and Carn Goedog with their evidence for quarrying of monoliths in the Middle Neolithic
126 period in the centuries before and up to c. 3000 BC (Parker Pearson et al., 2015, 2019).

127 Excavations at Waun Mawn in 2017–2021 revealed empty stoneholes for another eight
128 standing stones which had been erected to form an incomplete ring 110 m in diameter
129 (Parker Pearson et al., 2021; Parker Pearson, 2022). The discovery of further pits, dug
130 around the circumference but which never held standing stones, provides evidence that the
131 circle was abandoned in mid-construction and left unfinished. Radiocarbon-dating of wood

132 charcoal and optically stimulated luminescence (OSL) dating of sediments within the
133 stoneholes provide a likely construction date of c. 3400–3200 cal BC. Dating of the eight
134 standing stones' removal is less precise, placing these events before 2120±520 BC, though
135 this work is still on-going.

136 Close comparisons between Waun Mawn and Stonehenge include their sharing of
137 entrance orientations towards midsummer solstice sunrise and Stonehenge's enclosing
138 ditch having the same diameter as the Waun Mawn circle. A further possible link between
139 Stonehenge Stone 62 and Waun Mawn was provided by the shape of one of the stoneholes
140 (stonehole 91; Parker Pearson et al., 2021). Dolerite fragments recovered from this
141 stonehole included one which has been thought to have become detached from the
142 monolith which originally stood in this hole (Parker Pearson et al., 2021, Fig. 8).

143 **4. Methods**

144 *4.1. Analysis*

145 Between 2017 and 2021 a series of outcrops of dolerite (both spotted and non-spotted) in
146 the Mynydd Preseli in north Pembrokeshire were analysed by pXRF, whilst pXRF analyses
147 were performed during 2021 on the four large stones at Waun Mawn stone circle and two
148 dolerite fragments recovered from Waun Mawn stonehole 91. Analyses were performed
149 using a Thermo Fisher Scientific™ Niton™ XL3t Gold+ handheld XRF analyser. The Niton
150 pXRF uses a 2 W Ag anode X-ray tube, which can operate at between 6-50 kV and 0-200 μA,
151 with operating conditions being varied during the manufacturer-installed "TestAllGeo"
152 analysis method. This allows the instrument to determine a range of elements in geological
153 materials from Mg to U by use of different filters which operate in sequence together to
154 optimise sensitivity. The elements nominally determined in each mode are given in Table 1,
155 during a total analysis time of 100 s. An 8 mm diameter analysis spot (analysed area ~50
156 mm²) was used for all analyses, and the spectra were collected on a silicon drift detector,
157 processed and calibrated by the instrument's manufacturer-installed calibration.

158 *4.2. Accuracy of pXRF analyses*

159 To assess the accuracy of the Niton pXRF analyses, a series of reference materials (RMs)
160 have been analysed, including the NIST SRM 610 "Trace elements in Glass", Geological
161 Survey of Japan reference rocks JB-3 (Basalt) and JP-1 (Peridotite), and United States

162 Geological Survey CRM G-2 (Granite), taking reference values from published sources
163 (Flanagan, 1976; Govindaraju, 1994; Pearce et al., 1997; GeoReM, 2014). The analysed
164 concentrations from these RMs are presented in Supplementary Table 1. JB-3 and JP-1 were
165 prepared as standard 32 mm diameter XRF pressed powder pellets using 10 g of sample
166 pressed into a disk at 20 T with a few drops of Moviol® (PVA) binder. G-2, prepared in the
167 same way, was made as a 10 mm diameter pellet. JB-3 and JP-1 were also prepared as a
168 loose powder sample in a nylon holder, retained behind a Mylar® film as provided by Niton.
169 The accuracy of the RM analyses by pXRF is variable; Rb, Sr, Zr, Ti, K are better than $\pm 10\%$
170 while Ba, Zn, Fe, Nb and Zn are within $\pm 25\%$ of accepted values in JB-3 and G-2 (when
171 detected) from standard XRF pressed powder pellets. Nickel is overestimated at low
172 concentrations (JB-3) and underestimated at very high concentrations (JP-1), associated
173 with a poor (slightly flat) calibration on the Niton instrument, probably related to relatively
174 low sensitivity of the Ni K α line and an interference from Fe K β radiation on the background.
175 In G-2, Ni, which is well below the detection limits in basalts at 20-30 ppm, is recorded at
176 about 55 ppm, over 10 times its reference concentration of <5 ppm. The “Niton” standards
177 show slightly better analyses for some elements in JB-3, but worse in JP-1. The NIST glass, a
178 3 mm wafer about 15 mm in diameter containing about 450 ppm of most trace elements,
179 gave accurate analyses for Ca, Ti, Rb, Sr, Sn, Pb and U ($<\pm 10\%$) while Zr, Nb and V were
180 within $\pm 25\%$, but some elements were determined very poorly, including Ba and Cr, both
181 analysed at less than 5% of their true concentrations, presumably a reflection of the
182 complexity introduced into the background X-ray spectrum from a material with non-
183 geological concentrations of similar atomic number trace elements emitting X-rays of similar
184 wavelengths to these elements. Overall, the trace elements Rb, Sr, Zr, Nb, Zn, Th, Ba, along
185 with Ti, K, Fe, V, and Ca, have an accuracy within $\pm 20\%$ in basalts and granites, and whilst by
186 no means perfect, this is acceptable for provenance studies using the same instrument. The
187 abundant major elements Al and Si are determined poorly and show marked differences
188 between the pressed powder XRF pellets and the Niton loose-powder samples, presumably
189 related to differences in the mass absorption of X-rays leaving the different density samples.
190 The pXRF also reports unrealistically high concentrations of Cd and Sc in all analyses, and the
191 presence of high concentrations of many unexpected elements (e.g. Hg, Au, Pd) which will
192 not be present at the reported concentrations. This attests to some calibration issues within
193 the Niton instrument, the high Cd possibly a result of interference from the Compton

194 scattering of the Ag X-ray source radiation, and the Sc possibly an interference from a Ca K β
195 line.

196 Supplementary Table 1 also shows repeat analyses of Preseli dolerite, from both a large
197 hand specimen with weathered and fresh surfaces from Carn Goedog performed 5 years
198 apart, and repeats of a field traverse from Carn Meini taken 2 years apart. There are only
199 small differences in these repeat analyses for elements used in our attempts to correlate
200 sources (within the expected heterogeneity of the sample, typically better than $\pm 5 - 10\%$,
201 see Pearce et al., 2022) and this indicates the long-term consistency of calibration of the
202 pXRF instrument.

203 To ensure day-to-day consistency of pXRF analyses, in analysis sessions during 2021 a
204 piece of obsidian from the Big Obsidian Flow (BOF) at Newberry Volcano, Oregon was
205 analysed repeatedly to monitor the pXRF calibration. In Supplementary Table 2 we present
206 BOF results from different analytical sessions during 2021 which did not change significantly
207 during this study, meaning data from different sessions can be compared. For the analyses
208 of the Newberry BOF, day-to-day precision is good for the elements Rb, Zr, Sr, Nb, K, Ca, Al
209 and Fe (coefficient of variation, CV, from 5 analyses $\sim 3-4\%$), less good for Ba and Mn (CV
210 $\sim 8\%$) and lower again for Th and U (CV $\sim 8-13\%$), but all are within the range of all BOF
211 analyses performed as part of our provenance investigations. Some published averages for
212 analyses of the Newberry BOF are also presented in Supplementary Tables 1 and 2 (Laidley
213 and McKay, 1971; Higgins, 1973) and show that the pXRF results (taken from a single sample
214 of the flow) are in good agreement for some elements (Ba, Zr, Mn, Ca, K), again suggesting
215 acceptable accuracy (within $\pm 20\%$).

216 In pXRF analysis, limits of detection (LoD) vary from sample to sample, depending upon
217 the X-ray intensity received at the detector, and this is affected by many factors, including
218 sample composition (the effect of other elements in the same matrix) and analyser/sample
219 geometry. The instrument software calculates the LoD as 3 times the standard deviation of
220 the measurement, and no concentrations for those elements falling below the analysis LoD
221 are reported. Many elements are $< \text{LoD}$ in almost all samples analysed in this study (e.g. Se,
222 Te, Au, As, Hg), but others may be close to the LoD in some samples but not in others (e.g.
223 Ni with an LoD around 30 ppm in basaltic compositions). However, this non-reporting of

224 data provides some useful information on the general composition of a sample, suggesting
225 the distribution of low concentrations in a population.

226 Many authors have commented on issues related to pXRF analysis, including amongst
227 other issues spectral overlaps causing incorrect element identification, detection and
228 calibration, sample homogeneity and analysed spot size issues, attenuation of signal from
229 pore water or sample wetness, and surface weathering effects (Jones et al., 2005; Potts et
230 al., 2006; Hunt and Speakman, 2015). We have discussed these issues in earlier publications
231 related to provenance studies at Stonehenge using data obtained by pXRF (Bevins et al.,
232 2022; Pearce et al., 2022) and have developed an approach for analysis of heterogeneous,
233 coarse-grained dolerites which has been applied here, and which conforms to suggestions
234 made in other studies of similar material (Jones et al., 2005; Potts et al., 2006). In such
235 heterogeneous materials, where possible, we perform 20 analyses per orthostat, and these
236 settle to an average composition varying by less than $\pm 5\%$ of the mean after about 15
237 analyses for most elements useful in discriminating sources (Pearce et al., 2022). For the
238 outcrops in the Mynydd Preseli, methods of analysis are described below (Sections 4.3 and
239 4.4).

240 There has been much heated debate about the accuracy and reproducibility of pXRF,
241 and whether in such provenance studies it should be viewed as an archaeological or
242 geochemical tool (Frahm, 2013a; Frahm, 2013b; Speakman and Shackley, 2013). For analyses
243 such as these, whilst the accuracy and precision of pXRF is by no means perfect, but where
244 sampling for geochemical analysis by bulk methods of archaeological materials is unrealistic
245 on conservation or other grounds, and where there are limits on sampling the source
246 outcrops, pXRF provides an ideal analytical tool for provenance studies, provided its
247 limitations are carefully considered during the data analysis and interpretation.

248 4.3. *Analyses of Preseli dolerites*

249 Analyses of field outcrops considered in this study in the Preseli were conducted
250 between July 2017 and November 2021, and included eight locations, namely Carn Goedog
251 (2017), Cerrigmarchogion (2017), Carn Meini (2017 and 2019), Cerrig Lladron (2021), Carn
252 Fach (2021), Garn Ddu Fach (2021), Carn Ddafad-las (2021) and Carnau Ysfa (2021). The
253 distribution of these outcrops is shown on Figure 1. Analyses on the outcrops were

254 performed as a series of horizontal traverses of 10 or 15 analyses at a given height above
255 ground level, with several traverses being performed through the vertical height of the
256 outcrop. These were spaced 0.5 to 1 m apart, to give between 60-175 analyses per outcrop
257 in total, the size of the outcrop and time available determining the specific analytical
258 strategy. Our approach has been described elsewhere, and is not repeated here (Pearce et
259 al., 2022), with analyses presented here all being conducted on dry days so that any effects
260 of surface water attenuating light element fluorescent X-ray signals were minimal. The large
261 number of analyses overcomes the heterogeneity of the dolerites caused by either their
262 spotted or ophitic character (Jones et al., 2005; Pearce et al., 2022). Figure 2 shows field
263 photographs of three outcrops in the western Mynydd Preseli in the vicinity of the Waun
264 Mawn stone circle (viz. Cerrig Lladron, Carn Fach and Carnau Ysfa) which are all non-spotted
265 dolerite. These outcrops display variously developed columnar jointing features, all have an
266 ophitically-mottled surface (see Figure 2e) and all display late-stage veining (Figure 2f), the
267 latter being avoided during the pXRF analyses.

268 4.4. *Analysis of Waun Mawn stones and stonehole fragments*

269 We conducted *in-situ* pXRF analyses of the stones at Waun Mawn during dry weather in
270 April 2021. Analysed surfaces were chosen to be free from lichen (which covers parts of
271 some stones), they were all weathered, but not coated in Fe-oxides, and free from deposits
272 of lanolin and dye from sheep scratching themselves on the stones. We performed between
273 10 – 34 analyses per stone, depending upon the size of the stone, with analyses following
274 traverses between the small cards visible on the surfaces of the stones in Figure 3 (e.g. on
275 Stone C we analysed between cards 9-10 and 10-11 in Figure 3d, but in the others analysed
276 between adjacent numbers, i.e. 1-2 on Stone A in Figure 3b, 3-4, 5-6 and 7-8 on Stone B in
277 Figure 3c, and 12-13, 14-15 and 16-17 on Stone D in Figure 3e).

278 Two dolerite fragments recovered from Waun Mawn stonehole 91 were analysed
279 subsequently in the laboratory, but the same methodology was used for these samples as
280 for the four Waun Mawn stones.

281 4.5. *Statistical methods*

282 The use of statistics in correlating archaeological materials to geological sources can
283 be helpful, such as Principal Component Analysis (PCA), including pXRF studies on obsidians

284 from an archaeological perspective (Campbell and Healey, 2016; Muškara and Konak, 2022)
285 or the use of other multivariate methods for obsidians (e.g. Schmuck et al., 2022), or for the
286 Stonehenge sarsens (Nash et al., 2020). Similar statistical approaches in matching volcanic
287 ash deposits to source volcanoes have been applied in tephra studies (Sarna-Wojcicki et al.,
288 1979; Perkins et al., 1995; Perkins et al., 1998; Lowe et al., 2017) but it has been shown that
289 these methods can also obscure the relationships in data where a mix of elements are used
290 which are determined with varying precisions, depending on the statistical approach, e.g.
291 electron probe microanalysis of tephra glasses for correlation/provenance studies (Pollard
292 et al., 2006; Pearce et al., 2008). Many of these statistical approaches are often better for
293 proving differences, rather than proving compositional equivalence (Pearce et al., 2008;
294 Lowe et al., 2017) but again this can be unclear. Oftentimes variations in one or two
295 elements, related to geological processes, can be crucial indicators of provenance,
296 variations which may become hidden when multivariate approaches involving many
297 elements are used, and a combination of approaches (compositional space on bivariate
298 compositional diagrams, T-tests, statistical distance analyses, PCA) can often yield the most
299 useful comparisons. It must be remembered that it is variation in the raw data which
300 underpins all statistical tests, and an understanding of the range and variation in the raw
301 data is of prime importance. We illustrate the different approaches below by first
302 attempting PCA to try to correlate the Waun Mawn stones with possible sources, attempts
303 which we refine using a geochemical approach to yield finally a robust correlation.

304 In addition, once we have defined the sources of the four remaining stones at Waun
305 Mawn, in the light of the suggestion that the Waun Mawn circle was dismantled and
306 removed to Stonehenge (Parker Pearson et al., 2021), we investigate the probability of
307 leaving the four stones at Waun Mawn from an original 12, if the selection process to
308 remove the stones was random, a process akin to pulling, at random, different coloured
309 balls from a bag.

310 **5. Results and discussion**

311 *5.1. Elements used for discrimination*

312 Our previous study using pXRF analyses to source Stone 62 from Stonehenge to Garn
313 Ddu Fach in the Mynydd Preseli (Pearce et al., 2022) showed the utility of comparing the
314 compositional space occupied by analyses from Stone 62 with analyses from individual

315 Preseli outcrops to discriminate potential sources. To this end, a selection of elements
316 which are determined reliably by pXRF, i.e., having acceptable accuracy (better than about
317 $\pm 20\%$) and precision (around $\pm 10\%$ in homogeneous materials) and relatively unaffected by
318 surface weathering (see Potts et al., 2006), provided useful discriminators. These elements
319 are K, Ti, V, Fe, Mn, Ni, Zn, Rb, Sr, Zr, Nb and Ba. Nickel provides a discrimination between
320 the spotted and non-spotted dolerites, the latter having higher Ni (Bevins et al., 2014;
321 Bevins et al., 2021b) and whilst the spotted dolerites have Ni which is often close to the
322 limits of detection in pXRF (around 30 ppm in these basaltic compositions), this lack of
323 detection in the spotted Group 1 and 3 dolerites can be useful as a discriminant. Combining
324 Ni and Ba data proved useful in discriminating many of the bluestone outcrops in the
325 Mynydd Preseli (Pearce et al., 2022) and this is shown in Figure 4 for the Waun Mawn
326 stones.

327 5.2. Waun Mawn stones

328 All four stones from Waun Mawn have a closely similar composition, occupying
329 overlapping Ba vs Ni fields, with Ni contents ranging from about 40-150 ppm, and Ba
330 between 200-400 ppm (Figure 4). Nickel in these samples is most probably related to the
331 presence of pseudomorphs of chlorite after olivine, as seen in other non-spotted dolerites
332 but not in the spotted dolerites, and Ba will most likely be associated with the feldspathic
333 component.

334 Parker Pearson et al. (2021) suggested that the non-spotted dolerite bluestone Stone 62
335 at Stonehenge may potentially have occupied stonehole 91 at Waun Mawn, based on the
336 coincidence of their sizes and shapes. Compositional data for Stone 62 from Stonehenge
337 (from Pearce et al., 2022) is also shown in Figure 4, as well as analyses from the small drill
338 core removed from Stone 62 (reported by Thorpe et al., 1991), alongside data from Waun
339 Mawn. It is clear that Stone 62 is markedly different from any of the Waun Mawn stones,
340 having notably higher Ba and a Ni distribution which peaks at higher concentrations (see
341 histograms in Figure 4) than the analysed stones from this site. Stonehenge Stone 62 has
342 recently been provenanced to Garn Ddu Fach, a small outcrop in the eastern Mynydd Preseli
343 (Pearce et al., 2022), 6.79 km to the east-southeast of Waun Mawn (see Figure 1).

344 Figure 5 shows Ba vs Ni for the four Waun Mawn stones (WM-A to WM-D) plotted as
345 fields compared with surface analytical data (determined by pXRF) for all analysed outcrops
346 from Mynydd Preseli. About one-sixth of the analyses from Carn Fach and Carnau Ysfa Ni
347 were below the detection limit for pXRF (around 30 ppm), thus the extent of the
348 compositional fields on Figure 5 must continue to lower Ni. In contrast, for the Waun Mawn
349 Stones and Cerrig Lladron only 3% of the Ni analyses fell below the LoD, thus these fields
350 closely represent the complete compositional space occupied by the data (see
351 Supplementary Table 3, Analyses falling below LoD). The general overlap of the composition
352 of Cerrig Lladron with the Waun Mawn stones is clear, with Ba having the same range, and
353 Ni rising to about 140 ppm in Cerrig Lladron, a little lower than the highest Ni shown by a
354 Waun Mawn stone (170 ppm Ni from a single WM-C analysis, ~25 ppm higher than the
355 three other WM stones). Comparing the WM stones against analyses from individual
356 outcrops in the Mynydd Preseli, Carn Fach has Ba contents which extend to much higher
357 concentrations (around 530 ppm) while Ni shows fewer high concentrations (>95 ppm).
358 Carnau Ysfa has a composition which is restricted to lower Ni contents than many of the
359 WM stone analyses (with only 1 analysis >95 ppm) but displays a similar range in Ba; hence
360 it occupies a sub-set of the compositional space occupied by the WM stones. The
361 outcrops of Carn Goedog, Cerrigmarchogion and Carn Meini in the eastern Mynydd Preseli
362 have compositions which extend from similar to much higher Ba than occurs in any WM
363 stone, but Carn Goedog and Carn Meini are relatively low in Ni. For Garn Ddu Fach and Carn
364 Ddafad-las, the Ba compositions are almost all higher than the WM stones, whilst the range
365 of Ni is similar. Cerrigmarchogion shows similar Ni to Garn Ddu Fach, Carn Ddafad-las and
366 the WM stones, although has higher Ba than the WM stones which is lower than the Ba in
367 Garn Ddu Fach and Carn Ddafad-las.

368 Table 2 shows the average composition of the four Waun Mawn stones compared to the
369 three near-by western Mynydd Preseli outcrops for those elements determined in the
370 majority of analyses. It is apparent that many of the average compositions of the outcrops
371 overlap at ± 1 standard deviation, although some elements show systematic differences in
372 composition, for example Fe and Mn which are both about 50% higher in the Waun Mawn
373 stones than the outcrops, potentially the result of weathering forming an Fe-oxide crust on
374 the stones (see Potts et al., 2006).

375 To investigate if the similarity between the WM stones and Cerrig Lladron could be seen
376 using a statistical approach, PCA (which had proved successful in previous studies using bulk
377 sample analyses by XRF, Bevins et al. 2014), was conducted using Minitab® v14, using a
378 covariance matrix for the elements Zr, Sr, Rb, Ni, Fe, Mn, V, Ti, Ba, K, and Nb, performed
379 with no modification of the data (i.e. no scaling or normalisation) for all the analysed
380 outcrops in the Mynydd Preseli and the four Waun Mawn stones. The summary PCA results
381 are presented in Supplementary Table 4. This included 486 from 955 analyses where all
382 elements were above the detection limits by pXRF. The principal components here are
383 dominated by Fe (in PC1), Ti and K (in PC2) and K and Ti (in PC3). Figure 6 presents a series
384 of plots for PC1, PC2 and PC3 from this analysis grouped similarly to Figure 5. The plots of
385 PC1 vs PC2 largely separate the exposures of Cerrigmarchogion, Carn Goedog and Carn
386 Meini from the Waun Mawn stones, and most of the other outcrops show variable degrees
387 of overlap with the Waun Mawn stones. For PC3 vs PC2, there is a substantial overlap of all
388 analyses from the Preseli outcrops with the Waun Mawn stones, and this selection of
389 elements offers little discrimination other than separating two of the spotted dolerite
390 outcrops (Carn Goedog and Carn Meini) from the non-spotted Waun Mawn stones, which
391 simply confirms the petrographic observations. The variations in Fe which dominate the PCA
392 are likely to be associated with weathering (see above and Potts et al. 2006).

393 The greatest degree of overlap in the PCA is shown by the Waun Mawn stones and
394 the three outcrops closest to the stone circle, namely Cerrig Lladron, Carn Fach and Carnau
395 Ysfa, and these similarities are noted also in the Ba vs Ni data. Based on these observations,
396 Student T-tests were performed (using all compositional data) to assess any similarities
397 between the Waun Mawn stones and these possible local sources, with results tabulated in
398 Supplementary Table 3. Where the probability generated by the T-test exceeds 0.05
399 ($p > 0.05$) the data cannot be separated at a 95% confidence level, and the samples cannot be
400 said to be drawn from different populations. Here, many similarities are noted between the
401 three outcrops in Cl, Mg (although in over 40% of cases Mg is not detected and this is
402 therefore unreliable), Ca, V, and Pd (which is again unreliable, see above). The two most
403 similar outcrops from the T-test results are Carnau Ysfa and Carn Fach, and this is reflected
404 in similar Ni ranges and an overlap in Ba in the Ni-Ba diagram. This supports the field
405 observations which suggest these outcrops are along-strike exposures of the same sill.

406 Comparison of the Waun Mawn stones with each outcrop show the same number
407 (six each) of elements with $p > 0.05$, although Cerrig Lladron has more “near misses” than the
408 other outcrops ($p > 0.01$). Only one element, Pb, has $p > 0.05$ for all outcrops, and Pb has been
409 suggested as an atmospheric contaminant in the Preseli dolerites by Potts et al. (2006).
410 Other elements with $p > 0.05$ include Mg, P, Al, Nb, Ba, K, Ca, Ti, Zr, Rb, and Ni. The T-tests do
411 not unequivocally identify one outcrop as a potential source for the Waun Mawn stones.
412 Principal component analysis, again on unscaled geochemical data, was repeated using this
413 set of elements, excluding Pb and also Mg as it is not detected in a large number of
414 analyses. The PCA here included 458 analyses where all elements were above detection
415 limits, and the results are presented in Figure 7. Again, this offers no clear discrimination of
416 the Waun Mawn stones from any of the analysed outcrops in the Mynydd Preseli, although
417 a broad discrimination is evident in the compositional space occupied by these stones and
418 outcrops in the bivariate plot of Ba vs Ni (Figure 5).

419 In this instance, applying PCA without consideration of the possible causes of
420 geochemical variation amongst the analyses, has not been able to assist in the provenancing
421 of the Waun Mawn stones.

422 5.3. *Investigation of the compositional data*

423 We now return to consider the compositional data, our primary source of
424 information for these materials. It is our contention that this should be the first data
425 investigated in provenance studies (see Pearce et al., 2008) where statistical approaches,
426 widely applied in many geoarchaeological studies, do not yield clear results, as shown
427 above. Figure 8 shows the compositional data for the elements Sr, Rb, Zr, Ba, Ni and K for
428 the four Waun Mawn stones A-D with each analytical traverse on each stone separated (see
429 Figure 3), alongside plots for the variation of each element against height within the
430 exposures of Carn Lladron, Carnau Ysfa and Carn Fach. This gives a clearer indication of the
431 ranges of composition in each stone, and through the thickness of the exposed Preseli
432 dolerite sills. Dotted lines on Figure 8 mark the compositional ranges from the four Waun
433 Mawn stones combined. In some cases (e.g., Ni and Rb) the lower line most likely reflects
434 the limit of detection for that element (~30 ppm for Ni, ~2 ppm for Rb) although the LoD
435 varies for each analysis (see discussion in Pearce et al., 2022). For example, in Waun Mawn
436 stone B there are many analyses where Rb is below detection limits, with only 2 analyses

437 detecting Rb in traverse T5-T6, and none in T3-T4, while Sr is detected in all analyses. These
438 elements were selected as experience shows different outcrops occupy different
439 compositional spaces (Pearce et al., 2022) which can be related to geochemical processes.
440 Strontium is compatible in plagioclase and will be concentrated in the more felsic
441 components of the magmas. Nickel is associated with the mafic component of the dolerites,
442 particularly olivine and pseudomorphs thereafter, produced during the low-grade
443 metamorphism of the dolerites (see Bevins et al., 1989), and provides a good discriminant
444 between Group 2 and Groups 1 and 3 dolerites in the Mynydd Preseli (Bevins et al., 2014).
445 Potassium and Rb are essentially incompatible in basaltic magmas and will build up during
446 the evolution of the magma, so that crystallisation will cause these to increase. They are
447 also soluble elements, and any hydrous metamorphism may mobilise/concentrate these.
448 Zirconium is also highly incompatible but is immobile and should be little modified by
449 metasomatism/metamorphism, although it will concentrate in any baddeleyite which is
450 present (see Bevins et al., 2014). Barium, weakly incompatible in plagioclase, in basic
451 magmas shows a behaviour similar to K and Rb, increasing in the more compositionally
452 evolved magmas, and will generally associate with the felsic component of the melt.
453 Strontium in many analyses is much higher in Carn Fach and Carnau Ysfa than the Waun
454 Mawn stones, and is higher in a few analyses from Cerrig Lladron, whilst the lower range of
455 Sr is similar for all three outcrops. The range of Rb in the Waun Mawn stones is
456 encompassed by all three outcrops, and whilst its distribution appears similar to Carnau
457 Ysfa, this outcrop lacks the highest Rb concentrations recorded in stones D and A. Zirconium
458 (and also Nb, not shown) is similar between all outcrops and the Waun Mawn stones with
459 the highest concentrations recorded from two Waun Mawn stones. Barium is very similar
460 between the Waun Mawn stones and Cerrig Lladron, with Carnau Ysfa showing a notably
461 lower range in Ba concentrations, and Carn Fach having many analyses which show higher
462 concentrations. The Ni concentrations in Carn Fach and Carnau Ysfa are lower than in the
463 Waun Mawn stones, which most closely resemble the range of Cerrig Lladron, and it must
464 be remembered that about one sixth of the Ni analyses in Carn Fach and Carnau Ysfa are
465 below the LoD of pXRF analyses. Potassium in the Waun Mawn stones similarly displays the
466 same concentration range as Cerrig Lladron, and the stones show more analyses with higher
467 concentrations than Carn Fach, which are also notably higher in K than Carnau Ysfa.

468 Taking the six elements (Ba, Sr, Zr, Rb, K, Ni) used in Figure 8, PCA (again using
469 unscaled data) was undertaken for the outcrops analysed; the results are presented in
470 Figure 9. The Waun Mawn stones show almost no overlap with non-spotted dolerites from
471 Garn Ddu Fach and Carn Ddafad Las, only a slight overlap with material from
472 Cerrigmarchogion (non-spotted), Carn Meini and Carn Goedog (both spotted), and the two
473 proximal outcrops Carnau Ysfa and Carn Fach. There is however a complete overlap of the
474 Principal Components for analyses from Waun Maun and from Cerrig Lladron. To investigate
475 whether the use of scaled data in the PCA calculation would alter the interpretation, the
476 data was scaled so that the average element composition = 0 and the standard deviation =
477 1, a widely used approach prior to PCA. The PCs shown in Figure 9 were replotted for the
478 scaled compositions using both a covariance and a correlation matrix, and these PC plots
479 presented in Supplementary Figures 1 and 2. No difference in the interpretation of the PCA
480 was forthcoming using scaled data when compared with the raw data: the plots showed the
481 same similarities and differences between the Waun Mawn stones and the various Preseli
482 outcrops.

483 Thus, the similarity in Principal Component Analysis for raw and scaled data, the
484 similarities in compositional space occupied by the analyses described above, alongside
485 their petrography strongly suggests the Waun Mawn stones were derived from Cerrig
486 Lladron.

487 To establish whether two flakes of non-spotted dolerite from stonehole 91 at Waun
488 Mawn were possibly fragments from Stonehenge Stone 62 they were also analysed by pXRF
489 and the data for these are included in Table 2 (samples Stonehole 91 WAU18 TR8 070/35
490 and 070/36) and presented in Figure 10. Both of these samples have an iron-rich weathering
491 crust and sample 070/36 is particularly intensely weathered (see Figure 8 in Parker Pearson
492 et al., 2021). It is apparent in Table 2 that these flakes show high Fe and Mn compared to all
493 analyses of the western Mynydd Preseli outcrops and also the Waun Mawn stones, but also
494 considerably higher Al, Si, V, Zr, Nb, and Ti, whilst Ca and Sr are lower, and K, Rb, Ba, Mg and
495 Ni are similar. The formation of a Fe- and Mn-rich oxide crust during sub-surface weathering
496 of dolerite is typical in soils of pH~6, as found in the Waun Mawn area (see UKSO, 2022). At
497 this pH, high field strength elements (HFSE) such as Zr can be strongly sorbed onto hydrous
498 ferric oxides (HFO) with Zr reaching concentrations of up 0.22 μmol per mmol Fe at ~pH 6

499 (equivalent to about 360 ppm in the HFO, Yu and Liu, 2005). The relationship between high
500 Fe and Zr is shown in Figure 10a, with clear enrichment in the oxidised surfaces of these
501 flakes compared to all analyses from dolerite outcrops in the Mynydd Preseli, and it is clear
502 that both Fe and Zr have increased over normal dolerite compositions. The elevated Nb
503 recorded here (see Table 2) maintains the Zr/Nb ratio of typical Preseli dolerites, and
504 suggests Nb also behaves in this manner, and is not fractionated from Zr during weathering
505 and HFO formation. Strontium, in contrast, has decreased (by perhaps 50% or more) with
506 increasing weathering (increasing Fe, Figure 10b), associated with leaching of this soluble
507 ion from plagioclase, and the same is true of Ca (not shown). However, Ni and Ba seem to
508 be unaffected by this weathering, with these elements showing concentrations typical of
509 the analyses of all outcrops in the Mynydd Preseli (Figures 10c and 10d). This attests to
510 markedly different behaviours of Sr and Ba (both Group II elements) and Fe and Ni
511 (transition metals) during the weathering process, and indicates the care needed in
512 interpreting compositional data from weathered artefacts. Figures 10e and 10f show Ba vs
513 Ni and Ba vs Sr from the two flakes of weathered dolerite from stonehole 91 at Waun Mawn
514 compared to the compositions of outcrops from the western Mynydd Preseli outcrops close
515 to Waun Mawn. The Ba and Ni concentrations are closely similar to Cerrig Lladron (though
516 Ni is below detection in sample 070/36), and the Ba vs Sr data, when allowance is made for
517 the likely reduction in Sr during weathering, are also very similar to Cerrig Lladron. The
518 flakes also clearly have Ba, Ni and Sr which are all notably lower than analyses from Stone
519 62 at Stonehenge, and this shows that neither of these are pieces removed from Stone 62.

520 **6. Summary of results**

521 From the above, it is clear that the four non-spotted dolerite standing stones
522 currently at Waun Mawn all have a composition which is closely similar (see Figures 4,
523 5,8,9), suggestive of a common or closely related source. They have a composition which is
524 significantly different from Stone 62 at Stonehenge (Pearce et al., 2022), this being a stone
525 which had been proposed as originally occupying stonehole 91 at Waun Mawn (Parker
526 Pearson et al., 2021), and which has been sourced subsequently to Garn Ddu Fach, in the
527 eastern Mynydd Preseli (Pearce et al., 2022).

528 The Waun Mawn stones differ markedly in composition from the dolerite outcrops in
529 the eastern Mynydd Preseli and differ petrographically from Carn Meini and Carn Goedog in

530 that they are non-spotted and contain compositionally different secondary minerals.
531 Cerrigmarchogion, Carn Ddafad-las and Garn Ddu Fach all extend to much higher Ba than
532 any analyses from the Waun Mawn stones, and hence all of these outcrops can be ruled out
533 as a possible source. However, the three outcrops which are local to Waun Mawn in the
534 western Mynydd Preseli, viz. Cerrig Lladron, Carn Fach and Carnau Ysfa all show moderate
535 to high Ni and low Ba (200-400 ppm) and display some compositional overlap with the
536 Waun Mawn stones, with these three outcrops being possible sources. Comparing the
537 compositional space occupied by these outcrops and the Waun Mawn stones, Cerrig Lladron
538 is by far the most similar, having the same range of compositions of Ba, Zr, Rb, Ni and K, and
539 similar Sr. Carnau Ysfa has a slightly lower range of Rb, Ni and Ba, notably lower K, higher Sr,
540 and similar Zr, while Carn Fach displays higher Sr and Ba, marginally higher Rb, somewhat
541 lower K and Ni, and similar Zr. Based on these compositional similarities and differences, we
542 propose Cerrig Lladron as the most likely source of the four extant stones at Waun Mawn.

543 Adopting an approach where PCA is used to attempt to discriminate sources without
544 any consideration of the geochemistry (simply treating the compositions of individual
545 orthostats or outcrops as a variable without consideration of the differences or causes
546 therefore exemplified by variations in the “compositional space” the data occupies), leads
547 to an initial PCA result where all stones and sources appear similar. This is because the
548 subtle differences between source compositions (range and distribution of the
549 compositions) is masked for those elements which allow some discrimination (e.g. Ba, Ni, Sr,
550 Rb, K, Zr related to geological processes and mineralogical differences) by elements which
551 may be variable for other reasons (analytical considerations, weathering etc). When the
552 selection of elements for PCA is based on variations which can be seen in the analytical data,
553 even if these are subtle and which are related to geological/geochemical processes, then a
554 successful discrimination between sources can be achieved and a correlation suggested with
555 some confidence.

556 **7. Can the composition of the stones removed from the Waun Mawn stone circle be**
557 **inferred?**

558 The majority of dolerite bluestones at Stonehenge are spotted dolerite. If some of
559 these were once erected at Waun Mawn and removed (from the eight now unoccupied
560 stone holes at Waun Mawn) to leave the four non-spotted dolerites at Waun Mawn, either

561 (i) any spotted dolerites originally present (up to a maximum of eight) were removed
562 deliberately or (ii) a mix of eight stones, including spotted and non-spotted dolerites, were
563 removed, by a random selection. If the latter option were the case (with random selection
564 of the removed stones) consideration of the probability of leaving four non-spotted
565 dolerites derived from Cerrig Lladron can suggest something about the possible composition
566 of the original Waun Mawn circle. The probability of leaving behind, by random selection,
567 four stones which all derived from Cerrig Lladron (this is termed “the outcome”) from a
568 starting collection of twelve stones which could have derived from more than one source
569 has been calculated. The methodology is the same as calculating the probabilities of
570 randomly removing coloured balls from a bag without replacement to leave a particular set
571 of balls. In probability this is termed a “dependent event”, where the first ball removed
572 changes the probability for what is picked second, giving a “conditional probability” (i.e.,
573 what is the probability of an outcome dependant on prior actions?). This derives from
574 Bayes’ theorem, and the method of calculation is explained in Supplementary Methods 1. At
575 Waun Mawn, eight stones must have been removed from the original twelve, to leave four
576 which are all from Cerrig Lladron. The probability of this outcome can be calculated by
577 removal of stones from a starting collection which can vary from, at one extreme, assuming
578 all removed stones were from Cerrig Lladron, to, at the other extreme, none were from
579 Cerrig Lladron. The calculated probabilities are given in Table 3. As would be expected, the
580 probability of randomly leaving four stones behind from Cerrig Lladron is a likely outcome if
581 the original mixture was dominated by Lladron material, but this becomes increasingly
582 unlikely as more “foreign” stones are included in the original collection, so that there is only
583 a 1 in 4 chance of the outcome if there were three foreign stones in the original twelve, a 1
584 in 7 chance with four foreign stones, and only a 1 in 33 chance starting with an equal mix of
585 stones (i.e. six from Cerrig Lladron, six from elsewhere). If the stones were removed by a
586 random selection, this strongly suggests that the original assemblage of the Waun Mawn
587 circle was dominated by stones from Cerrig Lladron, if not entirely from that source. If the
588 choice was however deliberate (to specifically remove all the spotted dolerite stones) then
589 the probability analysis is not appropriate as this was not a random selection. Of course, the
590 reasons why the eight stones were removed, how they were chosen, and by whom is
591 unlikely ever to be known.

592

593 **8. Conclusions**

594 Of the twelve standing stones that can be considered as original to the Waun Mawn
595 circle, the four which remain there are most likely sourced from Cerrig Lladron, just 2.37 km
596 to the southwest. This raises the possibility that all of Waun Mawn's standing stones may
597 have come from Cerrig Lladron which lies some 3.7km west of Cerrigmarchogion (the source
598 of Stone 45 and 7km west of Garn Ddu Fach (the source of Stone 62. However, it should be
599 noted that stone circles of this diameter are commonly built with standing stones from
600 more than a single source (e.g. Stanton Drew, Somerset [Burl 1999, 55], Long Meg and her
601 Daughters, Cumbria [Burl 1999, 38], and Ring of Brodgar, Orkney [Richards 2013, 105–7]). If
602 the missing stones did all come from Cerrig Lladron then Waun Mawn's relevance for the
603 initial construction of Stonehenge in 2995–2920 cal BC (Parker Pearson et al., 2020, 168)
604 may only have been in terms of the failed completion of what was intended as a major
605 Neolithic monument rather than in terms of its provision of Stonehenge's bluestones. Of
606 course, it should be remembered that the remaining eight stones at Waun Mawn are of
607 unknown lithology, removed at an as yet unconfirmed date in prehistory, and that only 44
608 of Stonehenge's estimated 81 bluestones have survived (Parker Pearson et al., 2020, 299).

609 Finally, putting to one side these unknowns, if it is assumed that Waun Mawn was
610 not the source of any of Stonehenge's bluestones, then it is entirely possible that bluestones
611 could have come direct to Stonehenge from their quarries. This would be consistent with
612 radiocarbon dates of 3020–2920 cal BC and 3270–2910 cal BC for the end of the quarrying
613 sequences at Carn Goedog and Craig Rhos-y-Felin respectively (Parker Pearson et al., 2019).
614 Alternatively, the bluestones might have been erected at one or more additional stone
615 circles that were entirely dismantled and have consequently remained undetected.

616 In summary, our findings lead to the following conclusions:

- 617 i). The four remaining dolerite monoliths at Waun Mawn were sourced locally, most
618 probably from Cerrig Lladron, some 2.37 km to the southwest of the stone circle.
- 619 ii). The analysis of two flakes of stone from stonehole 91 are compositionally different to,
620 and thus not pieces from, Stone 62 at Stonehenge.

621 iii). The weathered dolerite fragments from stonehole 91 are interpreted as also coming
622 from Cerrig Lladron.

623 iv). If removal of the missing eight stones at Waun Mawn was random, probability analysis
624 suggests that it is likely that the majority, if not all, of the missing stones were sourced from
625 Cerrig Lladron.

626

627 **Acknowledgements**

628 We thank the Barony of Cemaes for permission to analyse dolerite outcrops *in-situ* in the
629 Mynydd Preseli. English Heritage (Heather Sebire and Susan Greaney) and Historic England
630 (Helen Woodhouse) are thanked for providing permission and access to analyse *in-situ*
631 Stone 62 at Stonehenge and for supporting this research more generally. We are grateful to
632 helpful inputs from two anonymous reviewers and for the editorial support of Dr Ellery
633 Frahm; all helped to improve this contribution.

634

635 **Funding**

636 Excavations and archaeological research at Waun Mawn in 2017–2018 were funded by the
637 Gerda Henkel Stiftung (grant nos: AZ 11/V/17 & AZ 08/V/18), the Rust Family Foundation,
638 the NERC Radiocarbon Panel and Raw-Cut TV. Investigations of the Stonehenge bluestones
639 using pXRF is in part funded by a Leverhulme Emeritus Fellowship to REB.

640

641 **References**

642 Atkinson, R.J.C., 1956. Stonehenge. London: Hamish Hamilton.

643

644 Bevins, R.E., Ixer, R.A., Pearce, N.J.G., 2014. Carn Goedog is the likely major source of
645 Stonehenge doleritic bluestones: evidence based on compatible element geochemistry and
646 Principal Component Analysis. *Journal of Archaeological Science* 42, 179-193.

647

648 Bevins, R.E., Ixer, R.A., Pirrie, D., Power, M.R., Cotterell, T., Tindle, A.G., 2021a. Alteration
649 fabrics and mineralogy as provenance indicators; the Stonehenge bluestone dolerites and
650 their enigmatic “spots”. *Journal of Archaeological Science: Reports* 36, 102826.

651

652 Bevins, R.E., Ixer, R. A., Webb, P.C., Watson, J.S., 2012. Provenancing the rhyolitic and dacitic
653 components of the Stonehenge landscape bluestone lithology: new petrographical and
654 geochemical evidence. *Journal of Archaeological Science* 39 1005-1019.
655

656 Bevins, R.E., Lees, G.J., Roach, R.A., 1989. Ordovician intrusions of the Strumble Head-
657 Mynydd Preseli region: lateral extensions of the Fishguard Volcanic Complex. *Journal of the*
658 *Geological Society, London* 146, 113-123.
659

660 Bevins, R.E., Pearce, N.J.G., Ixer, R.A., 2011. Stonehenge rhyolitic bluestone sources and the
661 application of zircon chemistry as a new tool for provenancing rhyolitic lithics. *Journal of*
662 *Archaeological Science* 38, 605-622.
663

664 Bevins, R.E., Pearce, N.J.G., Ixer, R.A., 2021b. Revisiting the provenance of the Stonehenge
665 bluestones: Refining the provenance of the Group 2 non-spotted dolerites using rare earth
666 element geochemistry. *Journal of Archaeological Science: Reports* 38, 103083.
667

668 Bevins, R.E., Pearce, N.J.G., Ixer, R.A., Hillier, S., Pirrie, D., Turner, P., 2022. Linking derived
669 debitage to the Stonehenge Altar Stone using portable X-ray fluorescence analysis.
670 *Mineralogical Magazine* 86, 1-13. doi:10.1180/mgm.2022.22

671 Bevins, R.E., Pirrie, D., Ixer, R.A., O'Brien, H., Parker Pearson, M., Power, M.R., Shail, R.K.,
672 2020. Constraining the provenance of the Stonehenge 'Altar Stone': Evidence from
673 automated mineralogy and U-Pb zircon age dating. *Journal of Archaeological Science*, 120,
674 105188.
675

676 Burl, A., 1999. *Great Stone Circles*. Newhaven, CI: Yale University Press.
677

678 Campbell, S., Healey, E., 2016. Multiple sources: The pXRF analysis of obsidian from Kenan
679 Tepe, SE Turkey. *Journal of Archaeological Science: Reports* 10, 377-389.
680

681 Flanagan, F.J., 1976. Descriptions and analysis of eight new USGS rock standards. *US Geol.*
682 *Surv. Professional Paper* 840, 192.
683

684 Frahm, E., 2013a. Is obsidian sourcing about geochemistry or archaeology? A reply to
685 Speakman and Shackley. *Journal of Archaeological Science* 40, 1444-1448.
686

687 Frahm, E., 2013b. Validity of "off-the-shelf" handheld portable XRF for sourcing Near
688 Eastern obsidian chip debris. *Journal of Archaeological Science* 40, 1080-1092.
689

690 GeoReM, 2014. http://georem.mpch-mainz.gwdg.de/sample_query.asp.
691

692 Govindaraju, K., 1994. 1994 compilation of working values and sample descriptions for 383
693 geostandards. *Geostandards Newsletter* 18: 1-331.
694

695 Higgins, M.W., 1973. Petrology of Newberry volcano, central Oregon. *Geological Society of*
696 *America Bulletin* 84, 455-488.
697

698 Hunt, A.M., Speakman, R.J., 2015. Portable XRF analysis of archaeological sediments and
699 ceramics. *Journal of Archaeological Science* 53, 626-638.
700

701 Ixer, R.A., Bevins, R.E., 2010. The petrography, affinity and provenance of lithics from the
702 Cursus Field, Stonehenge. *Wiltshire Archaeological & Natural History Magazine* 103, 1-15.
703

704 Ixer, R.A., Bevins, R.E., 2011. Craig Rhos-y-felin, Pont Saeson is the dominant source of the
705 Stonehenge rhyolitic debitage. *Archaeology in Wales* 50, 21-31.
706

707 Ixer, R.A., Bevins, R.E., Pirrie, D., Turner, P., Power, M., 2020. 'No provenance is better than
708 wrong provenance': Milford Haven and the Stonehenge sandstones. *Wiltshire Archaeology
709 and Natural History Magazine* 113, 1-15.
710

711 Jones, M.C., Williams-Thorpe, O., Potts, P.J., Webb, P.C., 2005. Using field-portable XRF to
712 assess geochemical variations within and between dolerite outcrops of Preseli, South Wales.
713 *Geostandards and Geoanalytical Research* 29, 251-269.

714 Laidley, R.A., McKay, D.S., 1971. Geochemical examination of obsidians from Newberry
715 Caldera, Oregon. *Contributions to Mineralogy and Petrology* 30, 336-342.
716

717 Lowe, D.J., Pearce, N.J.G., Jorgensen, M.A., Kuehn, S.C., Tryon, C.A., Hayward, C., 2017.
718 Correlating tephras and cryptotephras using glass compositional analyses and numerical and
719 statistical methods: review and evaluation *Quaternary Science Reviews* 175, 1-44.
720

721 Muşkara, Ü., Konak, A., 2022. Characterization of the Obsidian Used in the Chipped Stone
722 Industry in Kendale Hecala. *Quaternary* 5, 3.
723

724 Nash, D.J., Ciborowski, T.J.R., Ullyot, J.S., Parker Pearson, M., Darvill, T., Greaney, S.,
725 Maniatis, G., Whitaker, K.A., 2020. Origins of the sarsen megaliths at Stonehenge. *Science
726 Advances* 6: eabc0133.
727

728 Parker Pearson, M., 2022. Archaeology and legend: investigating Stonehenge. *Archaeology
729 International* 23, 144–64.
730

731 Parker Pearson, M., Bevins, R., Ixer, R., Pollard, J., Richards, C., Welham, K., Chan, B.,
732 Edinborough, K., Hamilton, D., Macphail, R., Schlee, D., Simmons, E., Smith, M., 2015. Craig
733 Rhos-y-felin: a Welsh bluestone megalith quarry for Stonehenge. *Antiquity* 89, 1331–52.
734

735 Parker Pearson, M., Pollard, J., Richards, C., Welham, K., Casswell, C., French, C., Shaw, D.,
736 Simmons, E., Stanford, A., Bevins, R.E., Ixer, R.A., 2019. Megalithic quarries for Stonehenge's
737 bluestones. *Antiquity* 93, 45–62.
738

739 Parker Pearson, M., Pollard, J., Richards, J., Tilley, C., Welham, K., 2020. *Stonehenge for the
740 ancestors. Part 1: landscape and monuments*. Leiden: Sidestone.
741

742 Parker Pearson, M., Pollard, J., Richards, C., Welham, K., Kinnaird, T., Shaw, D., Simmons, E.,
743 Stanford, A., Bevins, R.E., Ixer, R.A., Ruggles, C., Edinborough, K., 2021. The original

744 Stonehenge? A dismantled stone circle in the Preseli hills of west Wales. *Antiquity* 95, 85-
745 103.

746 Pearce, N.J.G., Bendall, C.A., Westgate, J.A., 2008. Comment on "Some numerical
747 considerations in the geochemical analysis of distal microtephra" by A.M. Pollard, S.P.E.
748 Blockley and C.S. Lane. *Applied Geochemistry* 23, 1353-1364.

749 Pearce, N.J.G., Bevins, R.E., Ixer, R.A., 2022. Portable XRF investigation of Stonehenge
750 bluestone 62 and potential source outcrops in the Mynydd Preseli, west Wales. *Journal of*
751 *Archaeological Science: Reports*. <https://doi.org/10.1016/j.jasrep.2022.103525>

752 Pearce, N.J.G., Perkins, W.T., Westgate, J.A., Gorton, M.P., Jackson, S.E., Neal, C.R., Chenery,
753 S.P., 1997. A compilation of new and published major and trace element data for NIST SRM
754 610 and NIST SRM 612 glass reference materials. *Geostandards Newsletter* 21, 115-144.

755 Perkins, M.E., Brown, F.H., Nash, W.P., McIntosh, W., Williams, S.K., 1998. Sequence, age,
756 and source of silicic fallout tuffs in middle to late Miocene basins of the northern Basin and
757 Range province. *Bulletin of the Geological Society of America* 110, 344-360.

758 Perkins, M.E., Nash, W.P., Brown, F.H., Fleck, R.J., 1995. Fallout tuffs of Trapper Creek, Idaho
759 - a record of Miocene explosive volcanism in the Snake River Plain volcanic province.
760 *Bulletin of the Geological Society of America* 107, 1484-1506.

761 Pollard, A.M., Blockley, S.P.E., Lane, C.S., 2006. Some numerical consideration in the
762 geochemical analysis of distal microtephra. *Applied Geochemistry* 21, 1692-1714.

763 Potts, P., Bernardini, F., Jones, M., Williams-Thorpe, O., Webb, P., 2006. Effects of
764 weathering on in situ portable X-ray fluorescence analyses of geological outcrops: dolerite
765 and rhyolite outcrops from the Preseli Mountains, South Wales. *X-Ray Spectrometry: An*
766 *International Journal*, 35 8-18.

767 RCAHMW, 1925. *Inventory of the Ancient Monuments in Wales: VII County of Pembroke*.
768 London: HMSO.

769

770 Ramsay, A.C., Aveline, W.T., Hull, E., 1858. *Geology of Parts of Wiltshire and Gloucestershire*
771 (Sheet 34). London: HMSO.

772

773 Richards, C. (ed.), 2013. *Building the Great Stone Circles of the North*. Oxford: Windgather.

774

775 Sarna-Wojcicki, A.M., Bowman, H.W., Russell, P.C., 1979. Chemical correlation of some late
776 Cenozoic tuffs of northern and central California by neutron activation analysis of glass and
777 comparison with X-ray fluorescence analysis. 2330-7102, for sale by the Supt. of Docs., US
778 Govt. Print. Off. 1979.

779

780 Schmuck, N., Carlson, R.J., Reuther, J., Baichtal, J.F., Butler, D.H., Carlson, E., Rasic, J.T., 2022.
781 Obsidian source classification and defining "local" in early Holocene Southeast Alaska.
782 *Geoarchaeology* 37, 466-485.

783

784 Speakman, R.J., Shackley, M.S., 2013. Silo science and portable XRF in archaeology: a
785 response to Frahm. *Journal of Archaeological Science* 40, 1435-1443.
786
787 Thomas, H.H., 1923. The source of the stones of Stonehenge. *The Antiquaries Journal* 3,
788 239-60.
789
790 Thorpe, R.S., Williams-Thorpe, O., Jenkins, D.G., Watson, J., Ixer, R., Thomas, R., 1991. The
791 geological sources and transport of the bluestones of Stonehenge, Wiltshire, UK,
792 *Proceedings of the Prehistoric Society* 57, 103-157.
793
794 UKSO, 2022. UK Soil Observatory data, [https://www.bgs.ac.uk/map-viewers/uk-soil-
795 observatory-ukso/](https://www.bgs.ac.uk/map-viewers/uk-soil-observatory-ukso/)
796
797 Yu, W., Liu, C., 2005. Sorption of Zr^{4+} and Hf^{4+} onto hydrous ferric oxide and their
798 fractionation behaviours: An experimental study. *Acta Geologica Sinica-English Edition* 79,
799 343-348.
800
801
802

803 **Table captions**

804 **Table 1.** Operating conditions for the *TestAllGeo* procedure used to determine the composition of
 805 the samples. An 8 mm diameter spot on the sample was analysed (approx. 50 mm²). Those elements
 806 detected with each filter as listed by Niton are given in *italics* (Niton XL3t 900 Analyzer with GOLDD
 807 Technology Users Guide, Version 6.5), with the elements shown in **bold** being detected in the
 808 majority of analyses conducted here and considered in this study.

Table 1. Operating conditions for the TestAllGeo procedure used to determine the composition of the samples. Those elements nominally detected with each filter as listed by Niton are given in *italics* (Niton XL3t 900 Analyzer with GOLDD Technology Users Guide, Version 6.5), with the elements shown in **Bold** being those detected in the majority of analyses *and* reported in this study.

pXRF Filter Configuration "TestAllGeo" mode	Time (s)	Elements determined
Main Range	30	<i>Mo, Zr, Sr, U, Rb, Th, Pb, Se, As, Hg, Zn, W, Cu, Ni, Co, Fe, Mn</i> Zr, Sr, Rb, Pb, As, Zn, Ni, Fe, Mn
Low Range	30	<i>Cr, V, Ti, Sc, Ca, K, S</i> V, Ti, Ca, K, S
High Range	20	<i>Ba, Cs, Te, Sb, Sn, Cd, Ag, Pd, Nb, Bi, Re, Ta, Hf</i> Ba, Nb
Light Range	20	<i>Al, P, Si, Ca, K, Cl, S, Mg</i> Al, P, Si, Mg

809 **Table 2:** Average compositions determined by pXRF (all concentrations ppm) of the four Waun
 810 Mawn stones (A-D) and the 3 outcrops in the western Mynydd Preseli. Also included is the average
 811 of 4 analyses of late-stage veins cutting stone D at Waun Mawn, which have notably higher
 812 incompatible element concentrations. The %>LoD row records the percentage of the 428 analyses
 813 performed on these samples which were above the limit of detection, with only those elements
 814 detected in >50% of analyses considered here. Cr has been excluded because of calibration issues
 815 (see Pearce et al. 2022).
 816

Units %>LoD	n=		Zr ppm 100%	Sr ppm 100%	Rb ppm 88%	Pb ppm 99%	As ppm 83%	Zn ppm 100%	Ni ppm 91%	Fe wt 100%	Mn wt % 100%	V ppm 100%	Ti wt % 100%	Ca wt % 100%
WM-A	10	Avg. S.D.	57 23	178 33	7.0 3.1	26 4	13 4	68 8	111 29	7.16 0.66	0.12 0.02	157 35	0.37 0.10	4.11 1.69
WM-B	30	Avg. S.D.	115 28	163 25	4.1 0.8	61 24	22 10	79 11	86 20	7.42 1.16	0.14 0.03	249 58	0.83 0.24	3.30 0.63
WM-C	20	Avg. S.D.	56 24	185 23	3.6 1.0	21 7	12 9	66 15	103 30	7.58 1.00	0.11 0.02	172 38	0.29 0.12	3.58 0.98
WM-D	30	Avg. S.D.	114 34	182 16	4.9 1.2	36 14	12 4	70 14	87 22	6.83 1.08	0.13 0.02	211 37	0.73 0.24	4.69 0.74
WM-v	4	Avg. S.D.	441 21	237 30	n.d.	111 23	25 14	37 12	55 13	3.43 0.61	0.06 0.01	155 36	0.84 0.19	3.55 0.27
Stonehole 91	15	Avg. S.D.	362 91	119 20	7.9 6.1	10 3	10 0	156 18	83 15	11.4 1.66	0.25 0.07	306 100	1.07 0.30	2.52 0.57
Stonehole 91	3	Avg. S.D.	313 24	59 7	10 n=1	n.d.	n.d.	165 21	n.d.	10.8 0.61	0.21 0.02	360 33	1.30 0.11	1.33 0.23
Cerrig Lladron	115	Avg. S.D.	74 38	216 33	7.3 3.8	40 14	22 16	58 15	84 21	5.70 1.03	0.09 0.01	168 42	0.39 0.21	4.15 1.40
Carn Fach	87	Avg. S.D.	103 57	281 79	5.7 3.3	47 18	26 21	48 19	65 24	5.15 1.51	0.08 0.03	175 70	0.59 0.54	4.20 1.55
Carnau Ysfa	70	Avg. S.D.	85 51	216 64	5.5 2.8	47 24	32 24	37 12	62 19	4.52 1.00	0.07 0.02	168 41	0.54 0.32	4.46 1.21

817

818

819

Table 3. Probabilities of removing 8 stones from 12 originally at Waun Mawn from different starting mixtures to produce an outcome leaving 4 stones from Cerrig Lladron.

Table 3. Probabilities of removing 8 stones at random from 12 stones originally present at Waun Mawn, with different starting mixtures, to leave 4 stones which all derived from Cerrig Lladron. The method is explained in Supplemental Methods 1.

Starting assemblage

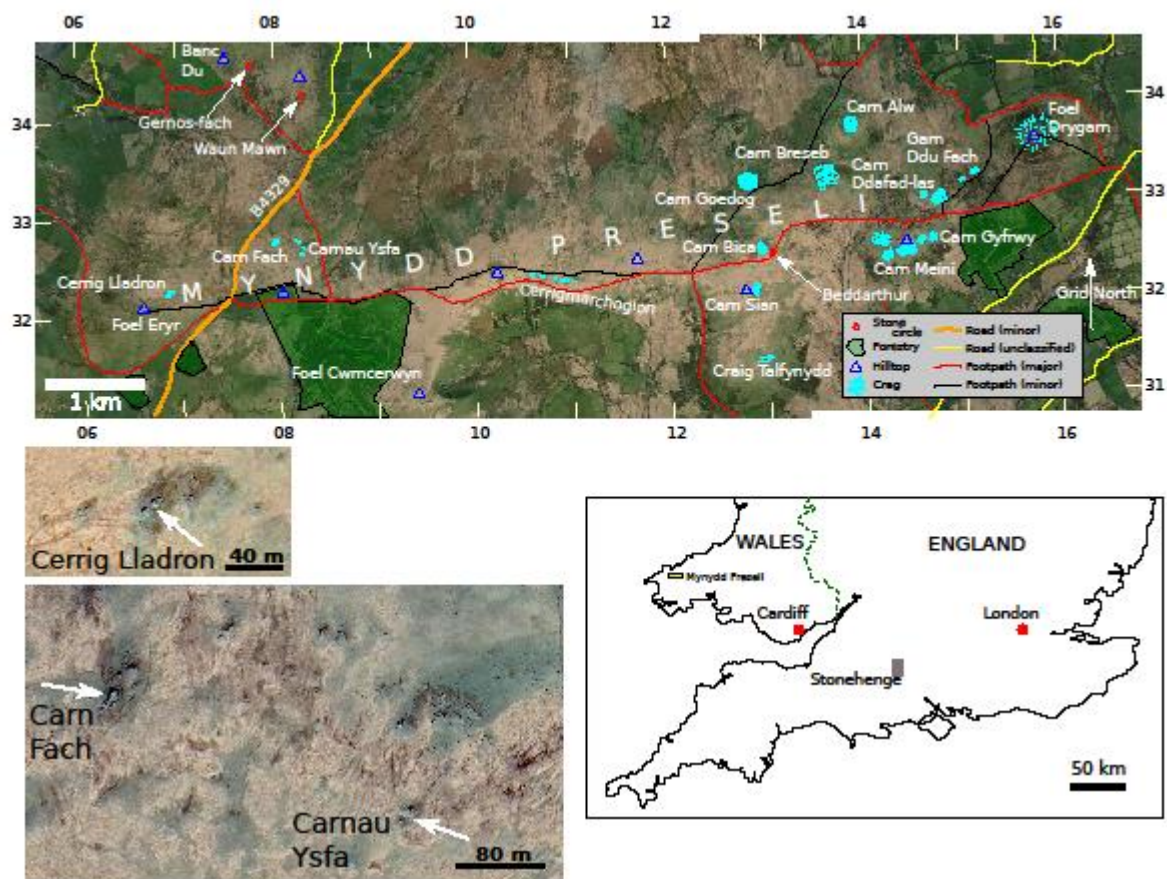
Cerrig Lladron stones	12	11	10	9	8	7	6	5	4
Non-Lladron stones	0	1	2	3	4	5	6	7	8

Probability after removal of 8 stones at random to leave 4 stones, all from Cerrig Lladron

p=	1	0.6667	0.4242	0.2545	0.1414	0.0707	0.0303	0.0101	0.0020
----	---	--------	--------	--------	--------	--------	--------	--------	--------

820
821

822 **Figure captions**



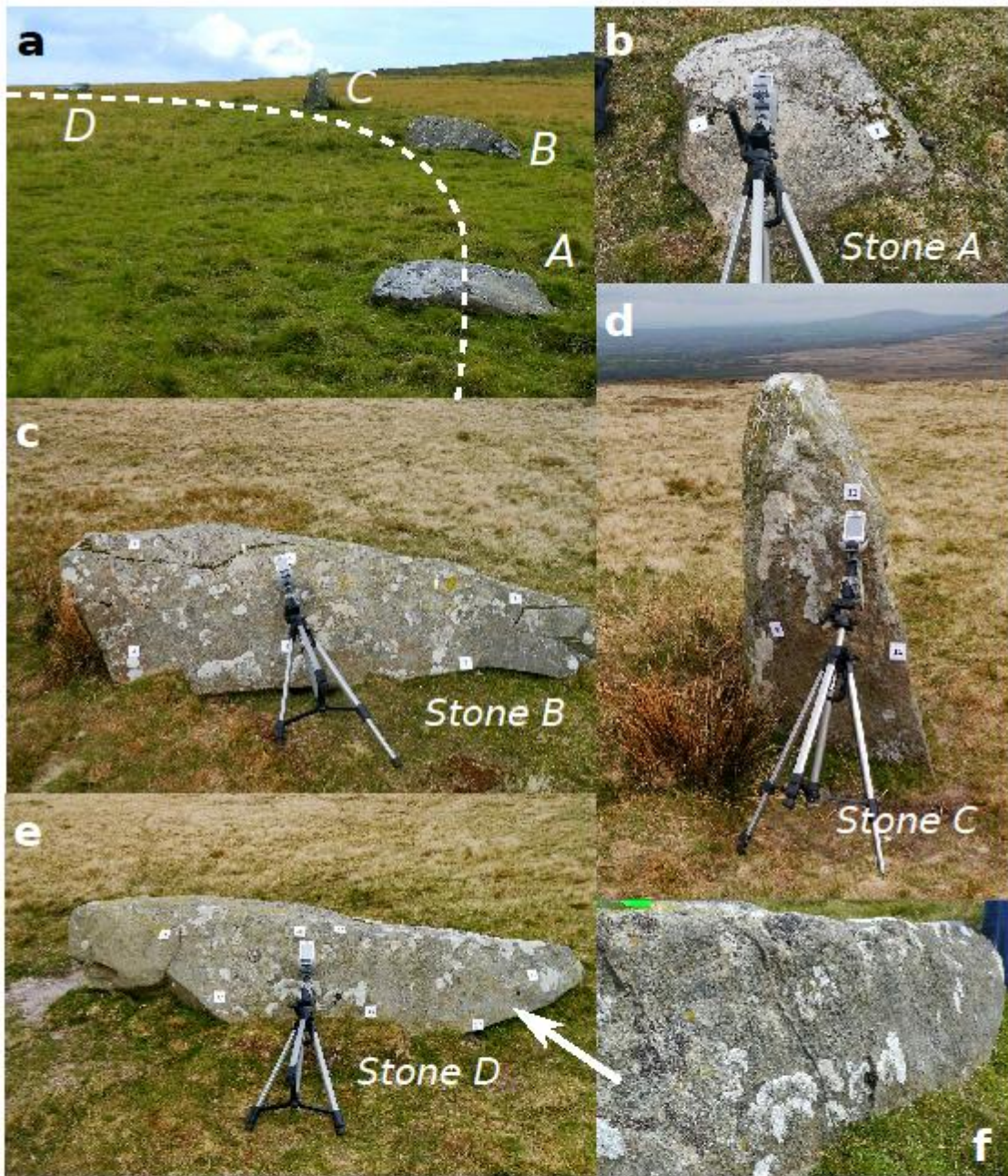
823
 824 **Figure 1:** Map of the Mynydd Preseli region showing the locations of the Waun Mawn and Gernos-
 825 fach stone circles, and the various outcrops of dolerite exposed in the area. Lower figures show the
 826 exposure of dolerite in the areas of Cerrig Lladron and Carn Fach/Carnau Ysfa, with arrows locating
 827 the analysed sections. Base image and insets © Google Earth with imagery from CNES/Airbus. Road

828 and other detail from Edina Digimap Ordnance Survey Service, from 1:50,000 Sheet SN02. ©Crown
829 copyright and database rights 2021 Ordnance Survey (100025252). Grid references refer to British
830 National Grid.



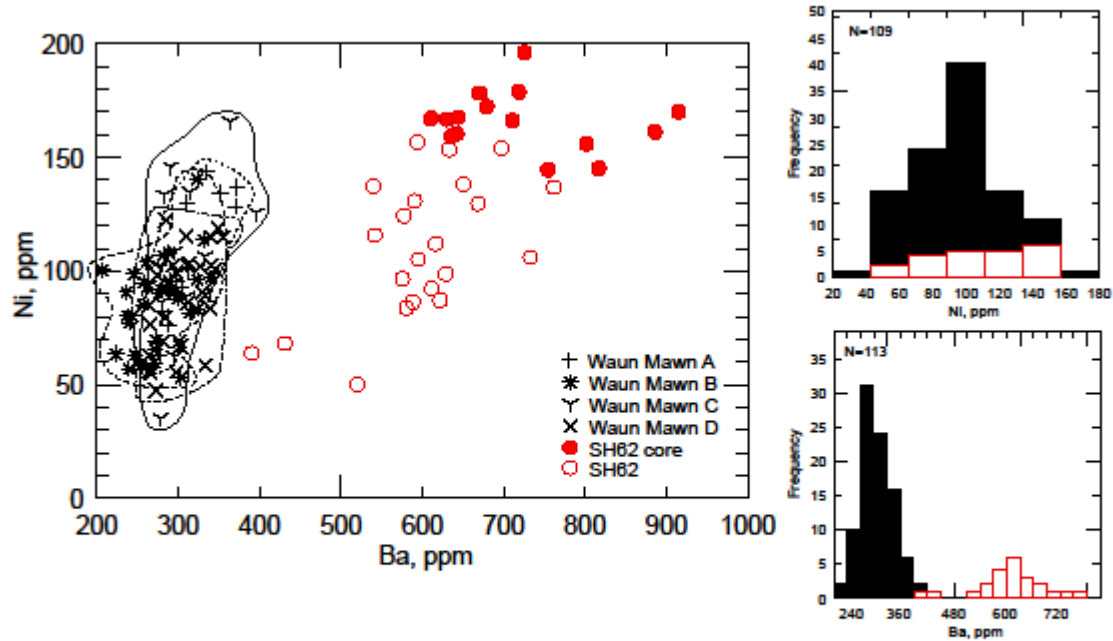
831 **Figure 2. a:** Carnau Ysfa. Waun Mawn is approximately 2 km to the N, on the hillside in the middle
832

833 distance, hidden behind the top of the outcrop above the pXRF. **b:** Carn Fach. Lies approximately 350
834 m WNW of Carnau Ysfa, view looking roughly NE. **c:** Cerrig Lladron. The arrow marks the position of
835 the Waun Mawn stone circle, approximately 2.3 km to the NE. **d:** A toppled block of dolerite showing
836 well developed columnar jointing at Cerrig Lladron. This block is behind the *in-situ* blocks in photo c.
837 **e:** The mottled weathered surface of the dolerite at Cerrig Lladron picking out the ophitic texture of
838 the dolerite – lens cap is 55 mm in diameter. **f:** Veins (varying from about 3 mm to 8 mm) cutting the
839 dolerite at Cerrig Lladron. For scale, in most pictures, the uppermost metal portion of the tripod leg
840 is 41 cm long.



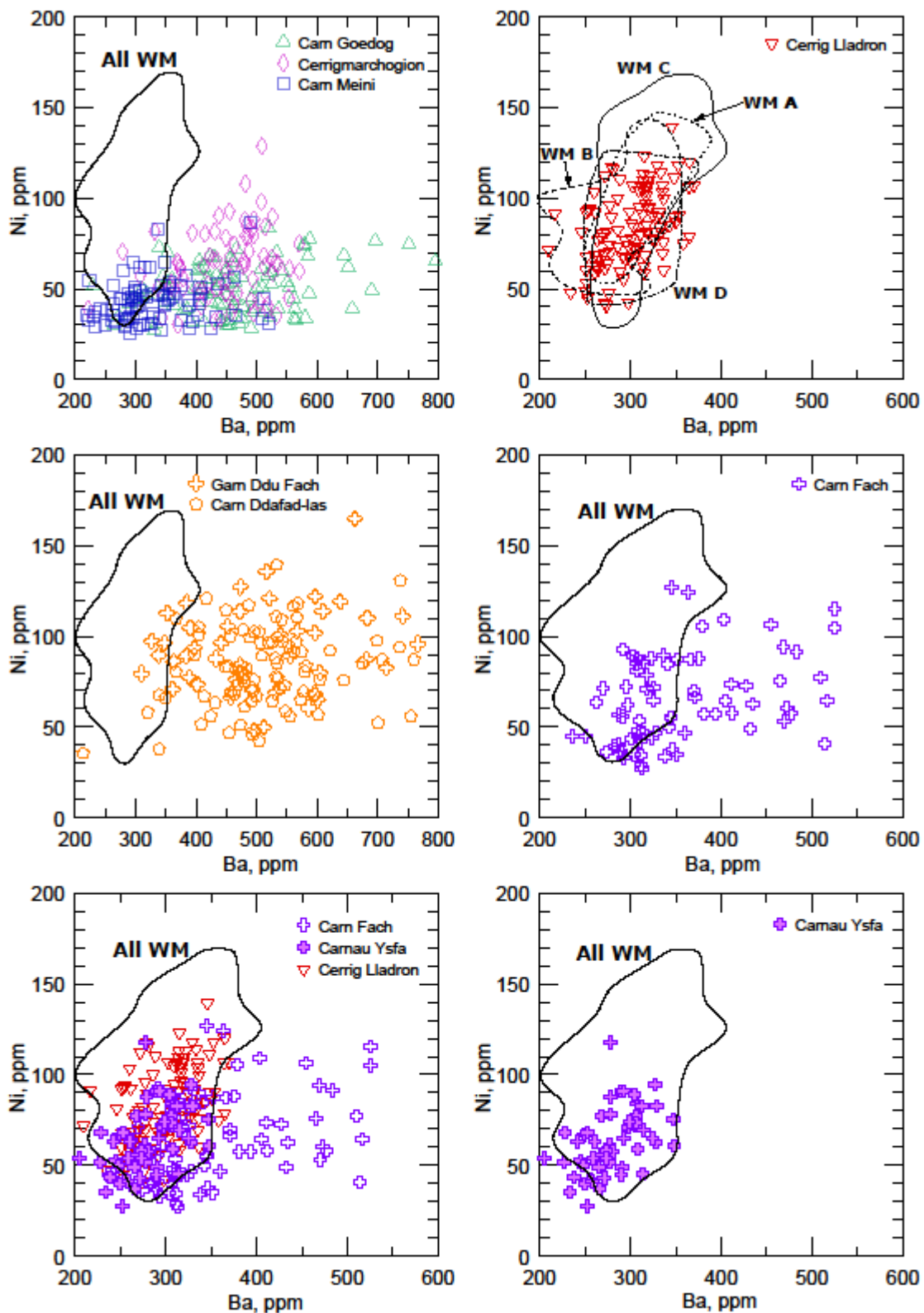
841
 842 **Figure 3:** The arc of former standing stones at Waun Mawn. **a:** General view looking roughly NW,
 843 with dotted line marking the approximate circumference of the circle; italic letters identify the
 844 stones. **b:** Analysed stone A (this is stone 13 from Parker Pearson et al., 2021, Fig. 2). **c:** Analysed
 845 stone B. **d:** Analysed stone C, the only remaining standing stone at Waun Mawn. **e:** Analysed stone

846 D. **f**: Oblique view showing detail of analysed stone D, picking out the mottled texture of the
847 weathered surface of the stone (centre of image), and the network of veins cutting the dolerite (left
848 of centre). The large lichens can be used to match the location in **e**. For scale, in most pictures, the
849 uppermost metal portion of the tripod leg is 41 cm long. Photos **a** and **f** courtesy of Amy Pearce.



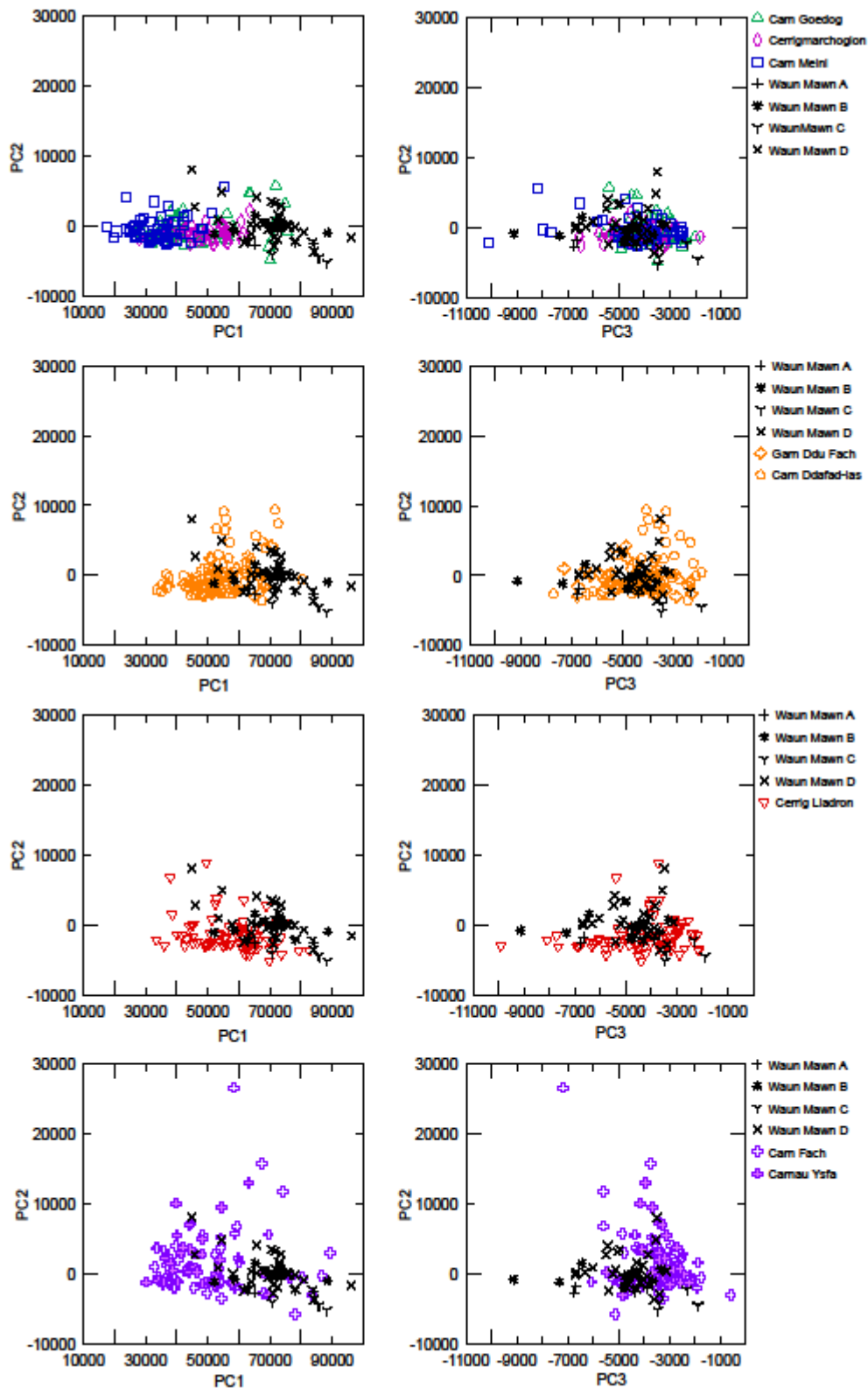
850
 851 **Figure 4:** Ba vs Ni (ppm) compositions (determined by pXRF) of analysed stones at Waun Mawn
 852 compared with the compositional data for Stone 62 (SH62) from Stonehenge, as both surface
 853 analyses (open circles) and as analyses of the core of SH62 (filled circles) taken by Thorpe et al.
 854 (1991). SH62 data from Pearce et al. (2022). Histograms show the differences in the distribution of

855 the Ba and Ni concentrations, for the surface analyses only (i.e. excluding the core from Stone 62),
856 with the Waun Mawn stones grouped together (in black) and SH62 the red boxes – frequency is the
857 total number of occurrences in both (combined) sets of data, and “N” is the number of analyses
858 above the LoD.



859
 860
 861
 862

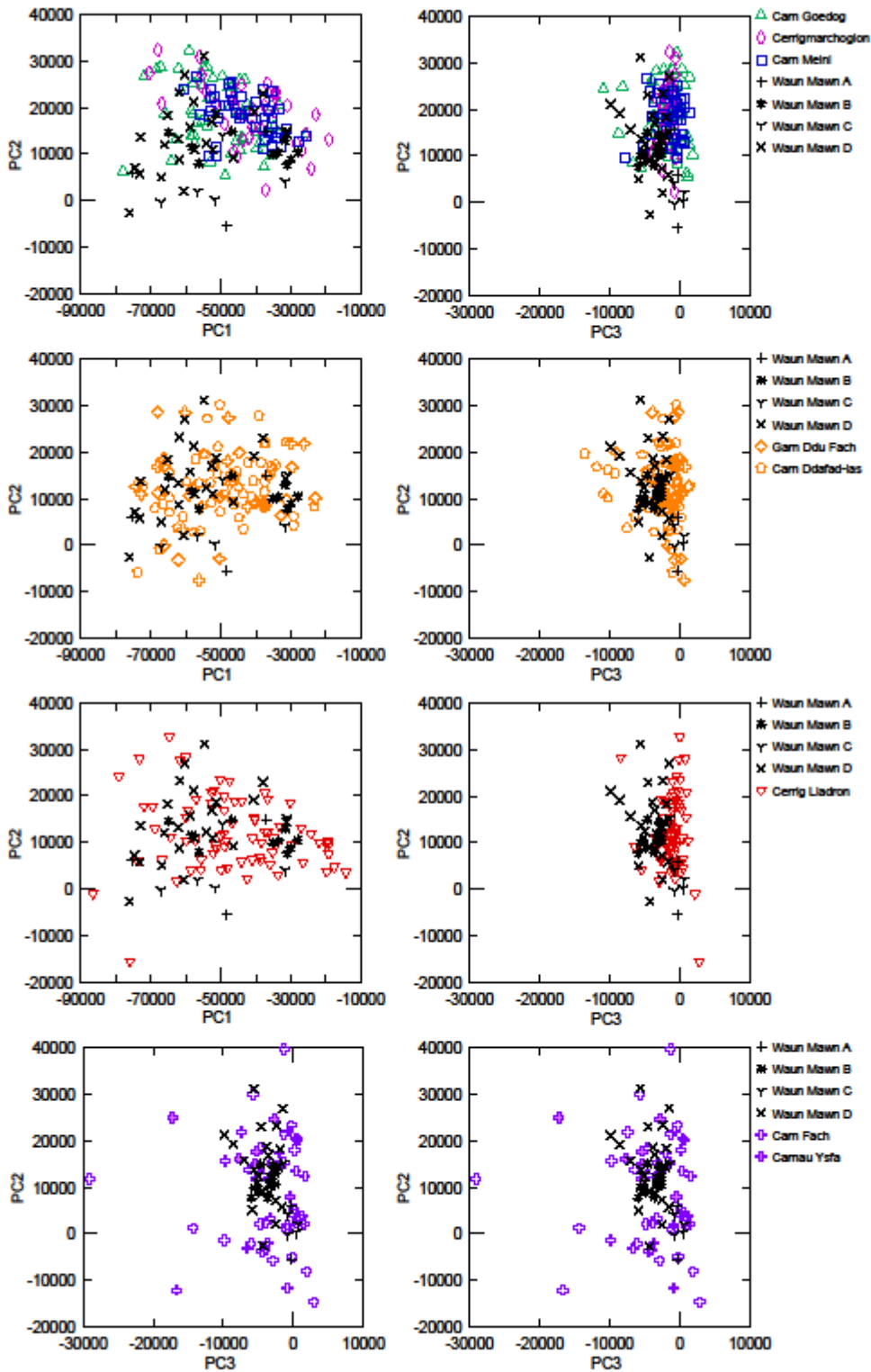
Figure 5: Ba vs Ni (ppm) for the Waun Mawn stones (plotted as fields) compared with data for all analysed outcrops from Mynydd Preseli, with the three outcrops closest to the Waun Mawn stone circle, Cerrig Lladron, Carn Fach and Carnau Ysfa, plotted separately. Note the different scales for Ba.



863
 864
 865
 866

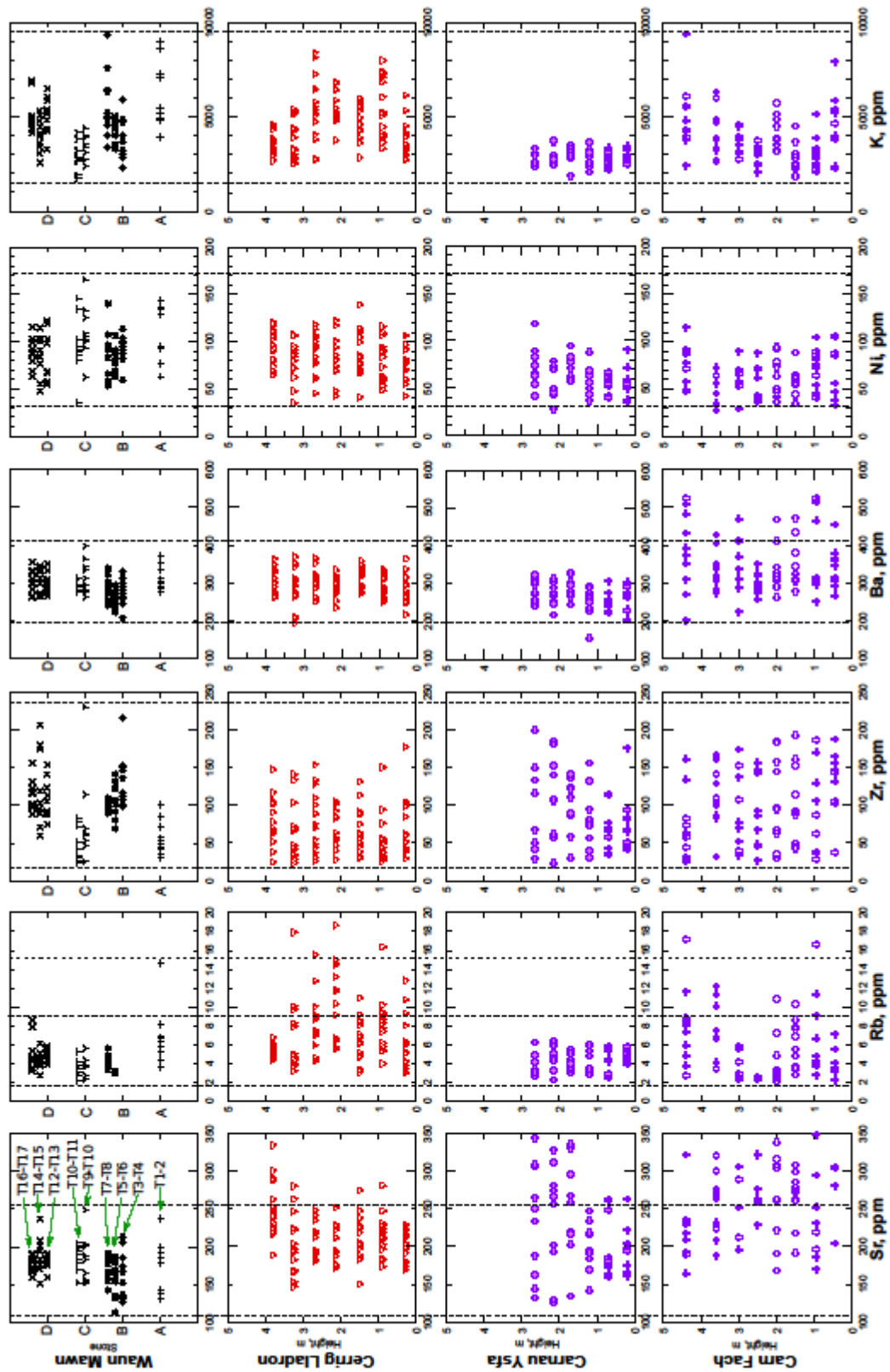
Figure 6: Plots of PC1, PC2 and PC3 from Principal Component Analysis of all analyses of the Waun Mawn stones and all analyses from outcrops in the Mynydd Preseli. These PCs represent 95%, 4.2% and 0.8% of the total variance respectively. PCA was performed in Minitab® v14.0 using Zr, Sr, Rb, Ni,

867 Fe, Mn, V, Ti, Ba, K, and Nb using a covariance matrix. Each row presents the PCs for a selection of
 868 the outcrops taken from the full PCA data set.



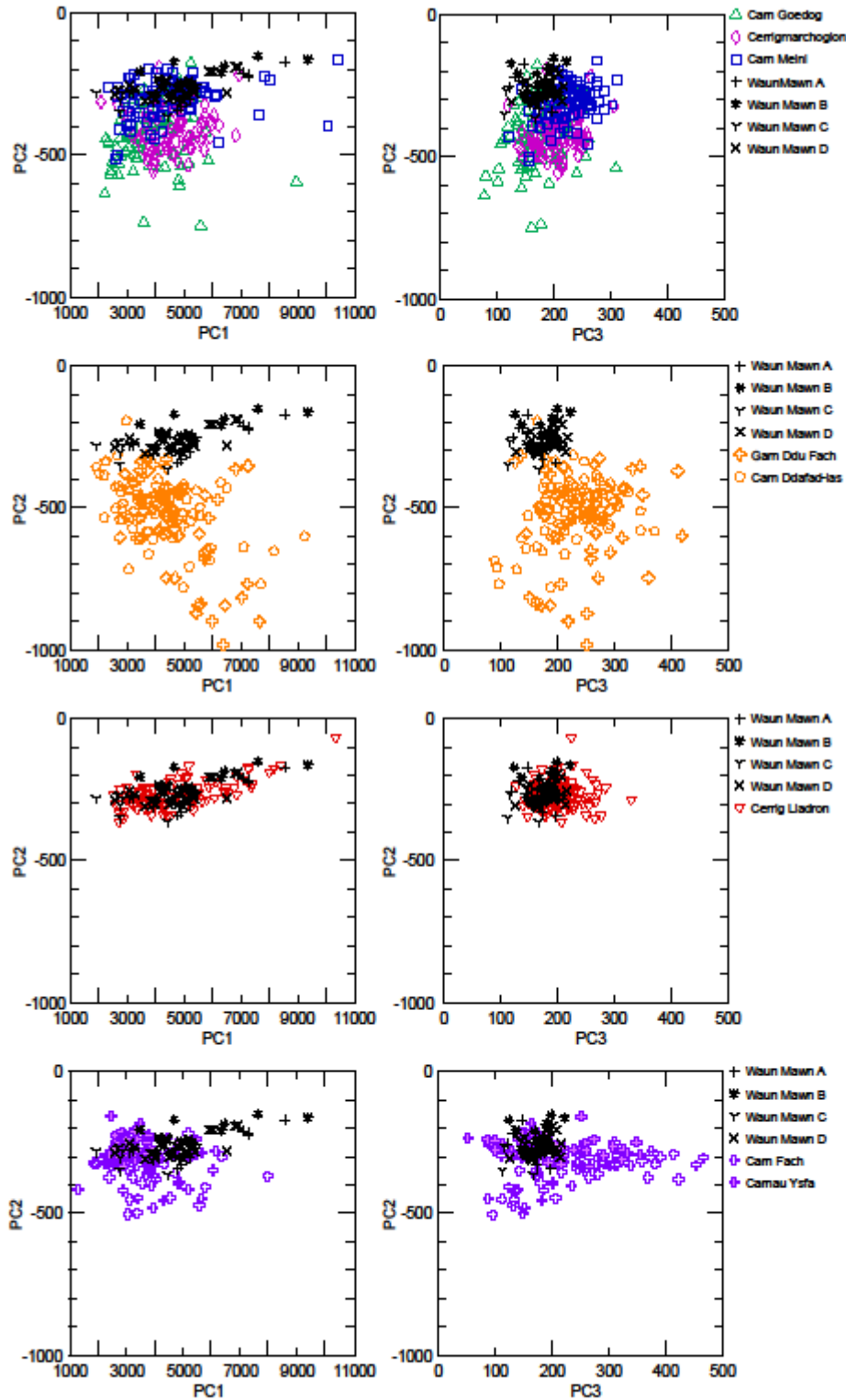
869
 870 **Figure 7:** Plots of PC1, PC2 and PC3 from Principal Component Analysis of all analyses of the Waun
 871 Mawn stones and all analyses from outcrops in the Mynydd Preseli. These PCs represent 69.1%,

872 26.8% and 3.5% of the total variance respectively. PCA was performed in Minitab® v14.0 using Zr,
 873 Rb, Ni, Ti, Ca, K, Ba, Nb, Al, and P using a covariance matrix. Each row presents the PCs for a selection
 874 of the outcrops taken from the full PCA data set.



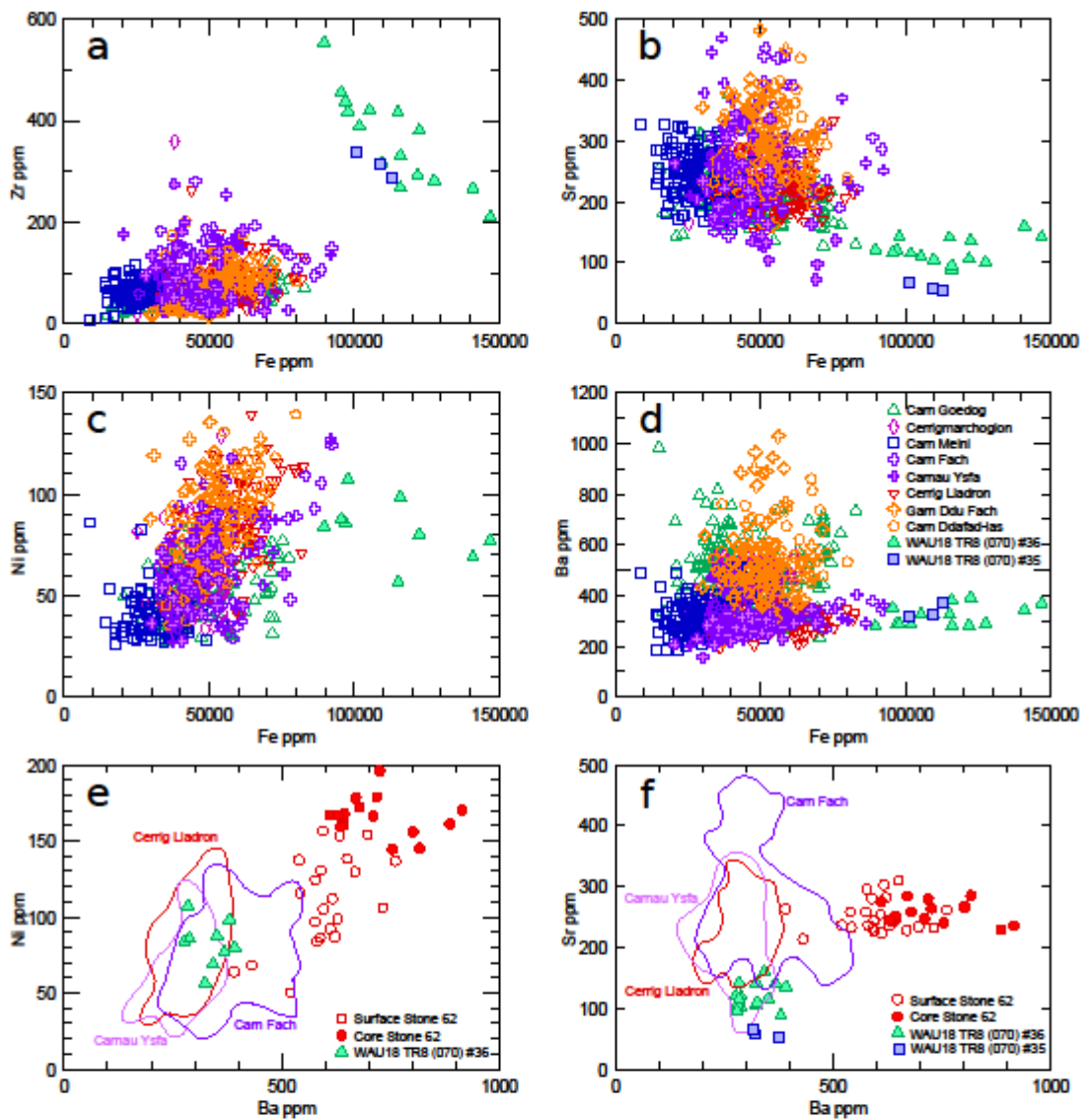
875
 876 **Figure 8:** Compositional data for the four Waun Mawn stones A-D for the elements Sr, Rb, Zr, Ba, Ni

877 and K (in ppm) compared with the variation of each element against stratigraphic height within the
 878 outcrops of Cerrig Lladron, Carnau Ysfa and Carn Fach. Each Waun Mawn stone is plotted separately,
 879 with each analytical traverse indicated. Symbols for the Waun Mawn stones as in Figure 4.



880
 881 **Figure 9:** Plots of PC1, PC2 and PC3 from Principal Component Analysis of all analyses of the Waun

882 Mawn stones and all analyses from outcrops in the Mynydd Preseli. These PCs represent 98.7%,
883 1.0% and 0.2% of the total variance respectively. PCA was performed in Minitab® v14.0 using Ba, Zr,
884 Sr, Rb, Ni, and K using a covariance matrix. Each row presents the PCs for a selection of the outcrops
885 taken from the full PCA data set.



886

887 **Figure 10: a-d.** Compositional variation in all analysed dolerites from the Mynydd Preseli compared
 888 to analyses of two weathered flakes of dolerite from stonehole 91 at Waun Mawn described by
 889 Parker-Pearson et al. (2021), plotted as Fe vs Zr, Sr, Ni and Ba respectively. Note Ni (LoD ~30 ppm by
 890 pXRF) was not detected in WAU18 TR8 (070) #35. All concentrations in ppm. e-f. Ba vs Ni and Ba vs

891 Sr (ppm) compositions of Stone 62 at Stonehenge (data from Pearce et al., 2022), the small core
892 taken from Stone 62 by Thorpe et al. (1991), and two weathered flakes of dolerite from stonehole 91
893 at Waun Mawn, with fields of data from the three western Mynydd Preseli outcrops. In Fig. e
894 WAU18 TR8 (070) #35 Ni is below the limits of detection by pXRF.